

Study of the exclusive $b \rightarrow u\ell^-\bar{\nu}_\ell$ decays in the MSSM with and without R-parity violation

C. S. Kim* and Ru-Min Wang†

Department of Physics, Yonsei University, Seoul 120-479, Korea

October 27, 2018

Abstract

We study the exclusive $b \rightarrow u\ell^-\bar{\nu}_\ell$ ($\ell = \tau, \mu, e$) decays in the MSSM with and without R-parity violation. From the experimental measurements of branching ratios $\mathcal{B}(B_u^- \rightarrow \tau^-\bar{\nu}_\tau)$, $\mathcal{B}(B_u^- \rightarrow M'^0\ell'^-\bar{\nu}_{\ell'})$ and $\mathcal{B}(\bar{B}_d^0 \rightarrow M'^+\ell'^-\bar{\nu}_{\ell'})$ ($\ell' = \mu, e$, $M' = \pi, \rho$), we derive new upper bounds on the relevant new physics parameters within the decays. Using the constrained new physics parameter spaces, we predict the charged Higgs effects and the R-parity violating effects on the branching ratios, the normalized forward-backward asymmetries of charged leptons, and the ratios of longitudinal to transverse polarization of the vector mesons, which have not been measured or have not been well measured yet. We find that the charged Higgs effects and the R-parity violating effects could be large and measurable in some cases. Our results could be used to probe new physics effects in the leptonic decays as well as the semileptonic decays, and will correlate with searches for direct supersymmetric signals in future experiments.

PACS Numbers: 13.20.He 12.60.Jv 14.80.Cp 11.30.Fs

*E-mail: cskim@yonsei.ac.kr

†E-mail: ruminwang@cskim.yonsei.ac.kr

1 Introduction

The rare B decays have received a lot of attention, since they are very promising for investigating the standard model (SM) and searching for new physics (NP) beyond it. Among these B decays, the rare semileptonic ones have played a central role for a long time, since the most precise measurements of the CKM matrix elements $|V_{ub}|$ and $|V_{cb}|$ are based on the semileptonic decays $b \rightarrow u\ell^-\bar{\nu}_\ell$ and $b \rightarrow c\ell^-\bar{\nu}_\ell$, respectively. These decays can also be very useful to test the various NP scenarios like the two Higgs doublet models [1], the minimal supersymmetric standard model (MSSM) [2, 3], and *etc.*

It is known that the charged Higgs boson exists in any models with two or more Higgs doublets, such as the MSSM which contains two Higgs doublets H_u and H_d coupling to up and down type quarks, respectively. The charged Higgs sectors of all these models may be characterized by the ratio of the two Higgs vacuum expectation values, $\tan\beta$, and the mass of the charged Higgs, m_H . Large $\tan\beta$ regime of both supersymmetric and nonsupersymmetric models has a few interesting signatures in B physics (for instance, see Refs. [4, 5, 6, 7, 8, 9, 10, 11, 12] and references therein). One of the most clear ones is the suppression of $\mathcal{B}(B_u^- \rightarrow \tau^-\bar{\nu}_\tau)$ with respect to its SM expectation [12]. In the MSSM, the charged Higgs contributions to the exclusive $b \rightarrow u\ell^-\bar{\nu}_\ell$ decays, including $B_u^- \rightarrow \tau^-\bar{\nu}_\tau$ decay, come from the b quark transforms to a u quark emitting a virtual charged Higgs that manifests itself as a lepton-neutrino pair. In this paper, we will present a correlated analysis of all these exclusive $b \rightarrow u\ell^-\bar{\nu}_\ell$ observables within the large $\tan\beta$ limit of the MSSM.

In the MSSM, one can introduce a discrete symmetry, called R -parity (R_p) [13], to enforce in a simple way the lepton number (L) and the baryon number (B) conservations. In view of the important phenomenological differences between supersymmetric models with and without R_p violation, it is also worth studying the extent to which R_p can be broken. The effects of SUSY with R_p violation in B meson decays have been extensively investigated, for instance Refs. [14, 15, 16, 17, 18, 19, 20]. In Ref. [20], the R_p violating (RPV) and lepton flavor violating coupling effects have been studied in $B^- \rightarrow \ell^-\bar{\nu}_\ell$ decays. The exclusive $b \rightarrow u\ell^-\bar{\nu}_\ell$ decays involve the same set of the RPV coupling products for every generation of leptons. In this work, still assuming lepton flavor conservation, we will investigate the sensitivity of the exclusive $b \rightarrow u\ell^-\bar{\nu}_\ell$ decays to the RPV coupling contributions in the RPV MSSM, too.

The paper is organized as follows. In section 2, we introduce the theoretical frame of the exclusive $b \rightarrow u\ell^-\bar{\nu}_\ell$ decays in the MSSM with and without R_p violation in detail. In section 3, we tabulate all the theoretical inputs. In sections 4 and 5, we deal with the numerical results. We display the constrained parameter spaces which satisfy all the available experimental data, and then we use the constrained parameter spaces to predict the NP effects on other quantities, which have not been measured or have not been well measured yet. Section 6 contains our summary and conclusion.

2 The exclusive $b \rightarrow u\ell^-\bar{\nu}_\ell$ decays in the MSSM with and without R-parity violation

In supersymmetric extensions of the SM, there are gauge invariant interactions which violate the B and the L in general. To prevent occurrences of these B and L violating interactions in supersymmetric extensions of the SM, the additional global symmetry is required. This requirement leads to the consideration of the so called R_p conservation (RPC).

In the MSSM with RPC, the terms in the effective Hamiltonian relevant for the $b \rightarrow u\ell^-\bar{\nu}_\ell$ decays are

$$\mathcal{H}_{eff}^{R_p}(b \rightarrow u\ell^-\bar{\nu}_\ell) = \frac{G_F}{\sqrt{2}}V_{ub}[(\bar{u}\gamma_\mu(1 - \gamma_5)b)(\bar{\ell}\gamma^\mu(1 - \gamma_5)\nu_\ell) - R_l(\bar{u}(1 + \gamma_5)b)(\bar{\ell}(1 - \gamma_5)\nu_\ell)], \quad (1)$$

here $R_l = \frac{\tan^2\beta}{m_H^2} \frac{\bar{m}_b m_l}{1 + \epsilon_0 \tan\beta}$, parameter ϵ_0 is generated at the one loop level (with the main contribution originating from gluino diagrams). Note that $\tilde{\epsilon}_0$ of [11] corresponds to ϵ_0 in our convention. The first term in Eq. (1) gives the SM contribution shown in Fig. 1(a), and the second one gives that of the charged Higgs scalars shown in Fig. 1(b).

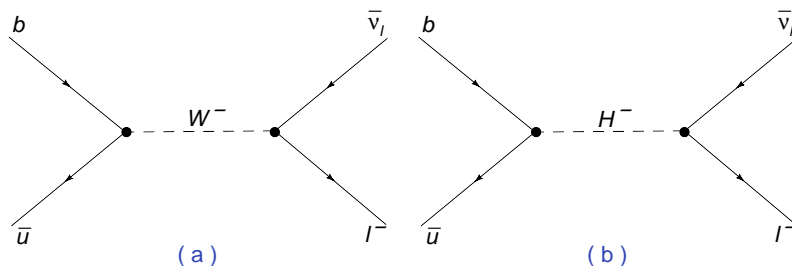


Figure 1: The decays $b \rightarrow u\ell^-\bar{\nu}_\ell$ are mediated by a W boson exchange in the SM, and in extensions of the SM also by a charged Higgs exchange.

Even though the requirement of RPC makes a theory consistent with present experimental searches, there is no good theoretical justification for this requirement. Therefore, the most general models with explicit R_p violation should be also considered. In the most general superpotential of the MSSM, the RPV superpotential is given by [21]

$$\mathcal{W}_{R_p} = \mu_i \hat{L}_i \hat{H}_u + \frac{1}{2} \lambda_{[ij]k} \hat{L}_i \hat{L}_j \hat{E}_k^c + \lambda'_{ijk} \hat{L}_i \hat{Q}_j \hat{D}_k^c + \frac{1}{2} \lambda''_{i[jk]} \hat{U}_i^c \hat{D}_j^c \hat{D}_k^c, \quad (2)$$

where \hat{L} and \hat{Q} are the SU(2) doublet lepton and quark superfields, respectively, \hat{E}^c , \hat{U}^c and \hat{D}^c are the singlet superfields, while i , j and k are generation indices and the superscript c denotes a charge conjugate field.

From Eq. (2), we can obtain the relevant four fermion effective Hamiltonian for the $b \rightarrow u_j \ell_m^- \bar{\nu}_{\ell n}$ processes with RPV couplings due to the squarks and sleptons exchange

$$\begin{aligned} \mathcal{H}_{eff}(b \rightarrow u_j \ell_m^- \bar{\nu}_{\ell n})^{R_p} &= - \sum_i \frac{\lambda'_{n3i} \lambda_{mji}^*}{8m_{\tilde{d}_{iR}}^2} (\bar{u}_j \gamma_\mu (1 - \gamma_5) b) (\bar{\ell}_m \gamma^\mu (1 - \gamma_5) \nu_{\ell n}) \\ &+ \sum_i \frac{\lambda_{im} \lambda_{ij3}^*}{4m_{\tilde{\ell}_{iL}}^2} (\bar{u}_j (1 + \gamma_5) b) (\bar{\ell}_m (1 - \gamma_5) \nu_{\ell n}). \end{aligned} \quad (3)$$

The corresponding RPV feynman diagrams for the $b \rightarrow u_j \ell_m^- \bar{\nu}_{\ell n}$ processes are displayed in Fig. 2. Note that the operators in Eq. (3) take the same form as those of the MSSM with RPC shown in Eq. (1).

Then, we can obtain the total effective Hamiltonian for the $b \rightarrow u \ell^- \bar{\nu}_\ell$ processes in the RPV MSSM

$$\begin{aligned} \mathcal{H}_{eff}^{R_p}(b \rightarrow u \ell^- \bar{\nu}_\ell) &\equiv \mathcal{H}_{eff}(b \rightarrow u \ell^- \bar{\nu}_\ell)^{\text{SM}} + \mathcal{H}_{eff}(b \rightarrow u \ell^- \bar{\nu}_\ell)^{R_p} \\ &= \left(\frac{G_F}{\sqrt{2}} V_{ub} - \sum_i \frac{\lambda'_{n3i} \lambda_{mji}^*}{8m_{\tilde{d}_{iR}}^2} \right) (\bar{u}_j \gamma_\mu (1 - \gamma_5) b) (\bar{\ell}_m \gamma^\mu (1 - \gamma_5) \nu_{\ell n}) \end{aligned}$$

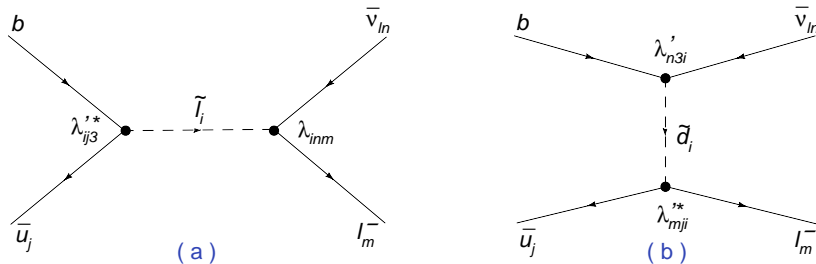


Figure 2: The RPV contributions to the exclusive $b \rightarrow u_j \ell_m^- \bar{\nu}_{\ell n}$ decays due to sleptons and squarks exchange.

$$+ \sum_i \frac{\lambda_{inm} \lambda_{ij3}^*}{4m_{\tilde{\ell}_{iL}}^2} (\bar{u}_j(1 + \gamma_5)b)(\bar{\ell}_m(1 - \gamma_5)\nu_{\ell n}). \quad (4)$$

Based on the effective Hamiltonian in Eq. (4), we will give the expressions of physical quantities for the RPV MSSM later in detail. Note that the operators in Eq. (4) have the exactly same form as those of the MSSM with RPC shown in Eq. (1). For the expressions of the charged Higgs contributions, we just need let $\sum_i \frac{\lambda'_{n3i} \lambda_{mji}^*}{8m_{\tilde{d}_{iR}}^2} = 0$ and replace $\sum_i \frac{\lambda_{inm} \lambda_{ij3}^*}{4m_{\tilde{\ell}_{iL}}^2}$ with $-\frac{G_F}{\sqrt{2}} V_{ub} R_l$. In the following expressions and numerical analysis, we will keep the masses of all three generation charged leptons, but ignore all neutrino masses.

2.1 The branching ratio for $B_u^- \rightarrow \ell^- \bar{\nu}_\ell$

$B_u^- \rightarrow \ell^- \bar{\nu}_\ell$ decay amplitude can be obtained in terms of Eq. (4),

$$\begin{aligned} \mathcal{M}^{\mathcal{H}_p}(B_u^- \rightarrow \ell^- \bar{\nu}_\ell) &= \langle \ell^- \bar{\nu}_\ell | \mathcal{H}_{eff}^{\mathcal{H}_p}(b \rightarrow u \ell^- \bar{\nu}_\ell) | B^- \rangle \\ &= \left[\frac{G_F}{\sqrt{2}} V_{ub} - \sum_i \frac{\lambda'_{n3i} \lambda_{m1i}^*}{8m_{\tilde{d}_{iR}}^2} \right] \langle 0 | \bar{u} \gamma_\mu (1 - \gamma_5) b | B^- \rangle \bar{\ell}_m \gamma^\mu (1 - \gamma_5) \nu_{\ell n} \\ &\quad + \sum_i \frac{\lambda_{inm} \lambda_{i13}^*}{4m_{\tilde{\ell}_{iL}}^2} \langle 0 | \bar{u} (1 + \gamma_5) b | B^- \rangle \bar{\ell}_m (1 - \gamma_5) \nu_{\ell n}. \end{aligned} \quad (5)$$

After using the definitions of B meson decay constant [22]

$$\langle 0 | \bar{u} \gamma_\mu \gamma_5 b | B^- \rangle = i f_{B_u} p_{B\mu}, \quad (6)$$

$$\text{and} \quad \langle 0 | \bar{u} \gamma_5 b | B^- \rangle = -i f_{B_u} \mu_{B_u} \quad \text{with} \quad \mu_{B_u} \equiv \frac{m_{B_u}^2}{m_b + m_u}, \quad (7)$$

we get the branching ratio for $B_u^- \rightarrow \ell^- \bar{\nu}_\ell$

$$\mathcal{B}^{\mathcal{H}_p}(B_u^- \rightarrow \ell^- \bar{\nu}_\ell) = \left| \frac{G_F}{\sqrt{2}} V_{ub} - \sum_i \frac{\lambda'_{n3i} \lambda_{m1i}^*}{8m_{\tilde{d}_{iR}}^2} + \sum_i \frac{\lambda_{inm} \lambda_{i13}^*}{4m_{\tilde{\ell}_{iL}}^2} \frac{\mu_{B_u}}{m_\ell} \right|^2 \frac{\tau_{B_u}}{4\pi} f_{B_u}^2 m_{B_u} m_\ell^2 \left[1 - \frac{m_\ell^2}{m_{B_u}^2} \right]^2. \quad (8)$$

From the above expression, we note that, unlike the contributions of squark exchange coupling $\lambda'_{n3i} \lambda_{m1i}^*$ and the SM to $\mathcal{B}(B_u^- \rightarrow \ell^- \bar{\nu}_\ell)$, slepton exchange coupling $\lambda_{inm} \lambda_{i13}^*$ is not suppressed by m_ℓ^2 .

2.2 The branching ratio for $B_{(s)} \rightarrow P \ell^- \bar{\nu}_\ell$ ($P = \pi, K$)

$B \rightarrow P \ell^- \bar{\nu}_\ell$ decay amplitude can be written as

$$\mathcal{M}^{\mathcal{H}_p}(B \rightarrow P \ell^- \bar{\nu}_\ell) = \langle P \ell^- \bar{\nu}_\ell | \mathcal{H}_{eff}^{\mathcal{H}_p}(b \rightarrow u \ell^- \bar{\nu}_\ell) | B \rangle$$

$$\begin{aligned}
&= \left[\frac{G_F}{\sqrt{2}} V_{ub} - \sum_i \frac{\lambda'_{n3i} \lambda_{m1i}^*}{8m_{d_{iR}}^2} \right] \langle P | \bar{u} \gamma_\mu (1 - \gamma_5) b | B \rangle \bar{\ell}_m \gamma^\mu (1 - \gamma_5) \nu_{\ell n} \\
&\quad + \sum_i \frac{\lambda_{inm} \lambda_{i13}^*}{4m_{\ell_{iL}}^2} \langle P | \bar{u} (1 + \gamma_5) b | B \rangle \bar{\ell}_m (1 - \gamma_5) \nu_{\ell n}.
\end{aligned} \tag{9}$$

Using the $B \rightarrow P$ transition form factors [22]

$$c_P \langle P(p) | \bar{u} \gamma_\mu b | B(p_B) \rangle = f_+^P(s) (p + p_B)_\mu + [f_0^P(s) - f_+^P(s)] \frac{m_B^2 - m_P^2}{s} q_\mu, \tag{10}$$

$$c_P \langle P(p) | \bar{u} b | B(p_B) \rangle = f_0^P(s) \frac{m_B^2 - m_P^2}{\bar{m}_b - \bar{m}_u}, \tag{11}$$

where the factor c_P accounts for the flavor content of particles ($c_P = \sqrt{2}$ for π^0 , and $c_P = 1$ for π^- , K^-) and $s = q^2$ ($q = p_B - p$), the differential branching ratio for $B \rightarrow P \ell^- \bar{\nu}_\ell$ is

$$\frac{d\mathcal{B}^{\mathcal{F}p}(B \rightarrow P \ell^- \bar{\nu}_\ell)}{ds d\cos\theta} = \frac{\tau_B \sqrt{\lambda_P}}{2^7 \pi^3 m_B^3 c_P^2} \left(1 - \frac{m_\ell^2}{s}\right)^2 [N_0^P + N_1^P \cos\theta + N_2^P \cos^2\theta], \tag{12}$$

$$\begin{aligned}
N_0^P &= \left| \frac{G_F}{\sqrt{2}} V_{ub} - \sum_i \frac{\lambda'_{n3i} \lambda_{m1i}^*}{8m_{d_{iR}}^2} \right|^2 [f_+^P(s)]^2 \lambda_P \\
&\quad + \left| \frac{G_F}{\sqrt{2}} V_{ub} - \sum_i \frac{\lambda'_{n3i} \lambda_{m1i}^*}{8m_{d_{iR}}^2} + \sum_i \frac{\lambda_{inm} \lambda_{i13}^*}{4m_{\ell_{iL}}^2} \frac{s}{m_\ell (\bar{m}_b - \bar{m}_u)} \right|^2 m_\ell^2 [f_0^P(s)]^2 \frac{(m_B^2 - m_P^2)^2}{s},
\end{aligned} \tag{13}$$

$$\begin{aligned}
N_1^P &= \left\{ \left| \frac{G_F}{\sqrt{2}} V_{ub} - \sum_i \frac{\lambda'_{n3i} \lambda_{m1i}^*}{8m_{d_{iR}}^2} \right|^2 + \text{Re} \left[\left(\frac{G_F}{\sqrt{2}} V_{ub} - \sum_i \frac{\lambda'_{n3i} \lambda_{m1i}^*}{8m_{d_{iR}}^2} \right)^\dagger \sum_i \frac{\lambda_{inm} \lambda_{i13}^*}{4m_{\ell_{iL}}^2} \frac{s}{m_\ell (\bar{m}_b - \bar{m}_u)} \right] \right\} \\
&\quad \times 2m_\ell^2 f_0^P(s) f_+^P(s) \sqrt{\lambda_P} \frac{(m_B^2 - m_P^2)}{s},
\end{aligned} \tag{14}$$

$$N_2^P = - \left| \frac{G_F}{\sqrt{2}} V_{ub} - \sum_i \frac{\lambda'_{n3i} \lambda_{m1i}^*}{8m_{d_{iR}}^2} \right|^2 [f_+^P(s)]^2 \lambda_P \left(1 - \frac{m_\ell^2}{s}\right), \tag{15}$$

where θ is the angle between the momentum of B meson and the charged lepton in the c.m. system of ℓ - ν , and the kinematic factor $\lambda_P = m_B^4 + m_P^4 + s^2 - 2m_B^2 m_P^2 - 2m_B^2 s - 2m_P^2 s$.

Here, we give the definition of the normalized forward-backward (FB) asymmetry of charged lepton [23], which is more useful from the experimental point of view,

$$\bar{\mathcal{A}}_{FB} = \frac{\int_0^{+1} \frac{d^2\mathcal{B}}{ds d\cos\theta} d\cos\theta - \int_{-1}^0 \frac{d^2\mathcal{B}}{ds d\cos\theta} d\cos\theta}{\int_0^{+1} \frac{d^2\mathcal{B}}{ds d\cos\theta} d\cos\theta + \int_{-1}^0 \frac{d^2\mathcal{B}}{ds d\cos\theta} d\cos\theta}. \tag{16}$$

Explicitly, for $B \rightarrow P \ell^- \bar{\nu}_\ell$ the normalized FB asymmetry is

$$\bar{\mathcal{A}}_{FB}(B \rightarrow P \ell^- \bar{\nu}_\ell) = \frac{N_1^P}{2N_0^P + 2/3N_2^P}. \tag{17}$$

2.3 The branching ratio for $B_{(s)} \rightarrow V\ell^-\bar{\nu}_\ell$ ($V = \rho, K^*$)

Similarly, the expression for $B \rightarrow V\ell^-\bar{\nu}_\ell$ decay amplitude is

$$\begin{aligned}
\mathcal{M}^{\mathcal{R}p}(B_u^- \rightarrow V\ell^-\bar{\nu}_\ell) &= \langle V\ell^-\bar{\nu}_\ell | \mathcal{H}_{eff}^{\mathcal{R}p}(b \rightarrow u\ell^-\bar{\nu}_\ell) | B^- \rangle \\
&= \left[\frac{G_F}{\sqrt{2}} V_{ub} - \sum_i \frac{\lambda'_{n3i} \lambda_{m1i}^*}{8m_{d_{iR}}^2} \right] \langle V | \bar{u}\gamma_\mu(1 - \gamma_5)b | B^- \rangle \bar{\ell}_m \gamma^\mu (1 - \gamma_5) \nu_{\ell n} \\
&\quad + \sum_i \frac{\lambda_{inm} \lambda_{i13}^*}{4m_{\ell_{iL}}^2} \langle V | \bar{u}(1 + \gamma_5)b | B^- \rangle \bar{\ell}_m (1 - \gamma_5) \nu_{\ell n}.
\end{aligned} \tag{18}$$

In terms of the $B \rightarrow V$ form factors [22]

$$\begin{aligned}
c_V \langle V(p, \varepsilon^*) | \bar{u}\gamma_\mu(1 - \gamma_5)b | B(p_B) \rangle &= \frac{2V^V(s)}{m_B + m_V} \epsilon_{\mu\nu\alpha\beta} \varepsilon^{*\nu} p_B^\alpha p^\beta \\
&\quad - i \left[\varepsilon_\mu^* (m_B + m_V) A_1^V(s) - (p_B + p)_\mu (\varepsilon^* \cdot p_B) \frac{A_2^V(s)}{m_B + m_V} \right] \\
&\quad + iq_\mu (\varepsilon^* \cdot p_B) \frac{2m_V}{s} [A_3^V(s) - A_0^V(s)],
\end{aligned} \tag{19}$$

$$c_V \langle V(p, \varepsilon^*) | \bar{u}\gamma_5 b | B(p_B) \rangle = -i \frac{\varepsilon^* \cdot p_B}{m_B} \frac{2m_B m_V}{\bar{m}_b + \bar{m}_u} A_0^V(s), \tag{20}$$

where $c_V = \sqrt{2}$ for ρ^0 , $c_V = 1$ for ρ^-, K^{*-} and with the relation $A_3^V(s) = \frac{m_B + m_V}{2m_V} A_1^V(s) - \frac{m_B - m_V}{2m_V} A_2^V(s)$, we have

$$\frac{d\mathcal{B}^{\mathcal{R}p}(B \rightarrow V\ell^-\bar{\nu}_\ell)}{ds d\cos\theta} = \frac{\tau_B \sqrt{\lambda_V}}{2^7 \pi^3 m_B^3 c_V^2} \left(1 - \frac{m_\ell^2}{s}\right)^2 [N_0^V + N_1^V \cos\theta + N_2^V \cos^2\theta], \tag{21}$$

$$\begin{aligned}
N_0^V &= \left| \frac{G_F}{\sqrt{2}} V_{ub} - \sum_i \frac{\lambda'_{n3i} \lambda_{m1i}^*}{8m_{d_{iR}}^2} \right|^2 \left\{ [A_1^V(s)]^2 \left(\frac{\lambda_V}{4m_V^2} + (m_\ell^2 + 2s) \right) (m_B + m_V)^2 \right. \\
&\quad + [A_2^V(s)]^2 \frac{\lambda_V^2}{4m_V^2 (m_B + m_V)^2} + [V^V(s)]^2 \frac{\lambda_V}{(m_B + m_V)^2} (m_\ell^2 + s) \\
&\quad \left. - A_1^V(s) A_2^V(s) \frac{\lambda_V}{2m_V^2} (m_B^2 - s - m_V^2) \right\} \\
&\quad + \left| \frac{G_F}{\sqrt{2}} V_{ub} - \sum_i \frac{\lambda'_{n3i} \lambda_{m1i}^*}{8m_{d_{iR}}^2} + \sum_i \frac{\lambda_{inm} \lambda_{i13}^*}{4m_{\ell_{iL}}^2} \frac{s}{m_\ell (\bar{m}_b + \bar{m}_u)} \right|^2 [A_0^V(s)]^2 \frac{m_\ell^2}{s} \lambda_V, \\
N_1^V &= \left\{ \left| \frac{G_F}{\sqrt{2}} V_{ub} - \sum_i \frac{\lambda'_{n3i} \lambda_{m1i}^*}{8m_{d_{iR}}^2} \right|^2 + \text{Re} \left[\left(\frac{G_F}{\sqrt{2}} V_{ub} - \sum_i \frac{\lambda'_{n3i} \lambda_{m1i}^*}{8m_{d_{iR}}^2} \right)^\dagger \sum_i \frac{\lambda_{inm} \lambda_{i13}^*}{4m_{\ell_{iL}}^2} \frac{s}{m_\ell (\bar{m}_b + \bar{m}_u)} \right] \right\} \\
&\quad \times \left[A_0^V(s) A_1^V(s) \frac{m_\ell^2 (m_B + m_V) (m_B^2 - m_V^2 - s) \sqrt{\lambda_V}}{sm_V} - A_0^V(s) A_2^V(s) \frac{m_\ell^2 \lambda_V^{\frac{3}{2}}}{sm_V (m_B + m_V)} \right]
\end{aligned} \tag{22}$$

$$+ \left| \frac{G_F}{\sqrt{2}} V_{ub} - \sum_i \frac{\lambda'_{n3i} \lambda_{m1i}^*}{8m_{d_{iR}}^2} \right|^2 A_1^V(s) V^V(s) 4s \sqrt{\lambda_V}, \quad (23)$$

$$N_2^V = - \left| \frac{G_F}{\sqrt{2}} V_{ub} - \sum_i \frac{\lambda'_{n3i} \lambda_{m1i}^*}{8m_{d_{iR}}^2} \right|^2 \left(1 - \frac{m_\ell^2}{s} \right) \lambda_V \left\{ [A_1^V(s)]^2 \frac{(m_B + m_V)^2}{4m_V^2} + [V^V(s)]^2 \frac{s}{(m_B + m_V)^2} + [A_2^V(s)]^2 \frac{\lambda_V}{4m_V^2 (m_B + m_V)^2} - A_1^V(s) A_2^V(s) \frac{m_B^2 - m_V^2 - s}{2m_V^2} \right\}, \quad (24)$$

where $\lambda_V = m_B^4 + m_V^4 + s^2 - 2m_B^2 m_V^2 - 2m_B^2 s - 2m_V^2 s$.

From Eq. (16), the normalized FB asymmetry of $B \rightarrow V \ell^- \bar{\nu}_\ell$ can be written as

$$\bar{\mathcal{A}}_{FB}(B \rightarrow V \ell^- \bar{\nu}_\ell) = \frac{N_1^V}{2N_0^V + 2/3N_2^V}. \quad (25)$$

For $B \rightarrow V \ell^- \bar{\nu}_\ell$ decay, besides the branching ratio and the normalized FB asymmetry of charged lepton, another interesting observable is the ratio of longitudinal to transverse polarization of the vector meson Γ_L^V/Γ_T^V , which can be derived from the following differential expressions

$$\begin{aligned} \frac{d\Gamma_L^{\mathcal{H}_p}}{ds} &= \frac{\sqrt{\lambda_V}}{2^7 \pi^3 m_B^3 c_V^2} \left(1 - \frac{m_\ell^2}{s} \right)^2 \left\{ \left| \frac{G_F}{\sqrt{2}} V_{ub} - \sum_i \frac{\lambda'_{n3i} \lambda_{m1i}^*}{8m_{d_{iR}}^2} \right|^2 \left(\frac{4}{3} + \frac{2m_\ell^2}{3s} \right) \right. \\ &\quad \times \left([A_1^V(s)]^2 \frac{(m_B^2 - m_V^2 - s)^2 (m_B + m_V)^2}{4m_V^2} \right. \\ &\quad \left. \left. + [A_2^V(s)]^2 \frac{\lambda_V^2}{4m_V^2 (m_B + m_V)^2} - A_1^V(s) A_2^V(s) \frac{(m_B^2 - m_V^2 - s) \lambda_V}{4m_V^2} \right) \right. \\ &\quad \left. + 2 \left| \frac{G_F}{\sqrt{2}} V_{ub} - \sum_i \frac{\lambda'_{n3i} \lambda_{m1i}^*}{8m_{d_{iR}}^2} + \sum_i \frac{\lambda_{inm} \lambda_{i13}^*}{4m_{\ell_{iL}}^2} \frac{s}{m_\ell (\bar{m}_b + \bar{m}_u)} \right|^2 [A_0^V(s)]^2 \frac{m_\ell^2}{s} \lambda_V \right\}, \quad (26) \end{aligned}$$

$$\begin{aligned} \frac{d\Gamma_T^{\mathcal{H}_p}}{ds} &= \frac{\sqrt{\lambda_V}}{2^7 \pi^3 m_B^3 c_V^2} \left(1 - \frac{m_\ell^2}{s} \right)^2 \left| \frac{G_F}{\sqrt{2}} V_{ub} - \sum_i \frac{\lambda'_{n3i} \lambda_{m1i}^*}{8m_{d_{iR}}^2} \right|^2 \frac{8}{3} \\ &\quad \times \left\{ [A_1^V(s)]^2 (m_\ell^2 + 2s) (m_B + m_V)^2 + [V^V(s)]^2 \frac{\lambda_V (m_\ell^2 + 2s)}{(m_B + m_V)^2} \right\}. \quad (27) \end{aligned}$$

In this section, we give the expressions of only the exclusive $b \rightarrow u \ell^- \bar{\nu}_\ell$ decays, but we will use the CP averaged results of the exclusive $b \rightarrow u \ell^- \bar{\nu}_\ell$ and $\bar{b} \rightarrow \bar{u} \ell^+ \nu_\ell$ decays in our numerical analysis.

3 Input Parameters

The input parameters except the form factors are collected in Table I. In our numerical results, we will use the input parameters, which are varied randomly within 1σ range.

Table I: Default values of the input parameters and the $\pm 1\sigma$ error ranges for the sensitive parameters used in our numerical calculations.

$m_{B_s} = 5.366$ GeV, $m_{B_d} = 5.279$ GeV, $m_{B_u} = 5.279$ GeV, $m_{K^{*\pm}} = 0.892$ GeV,	
$m_{\pi^\pm} = 0.140$ GeV, $m_{\pi^0} = 0.135$ GeV, $m_\rho = 0.775$ GeV, $m_{K^\pm} = 0.494$ GeV,	
$\overline{m}_b(\overline{m}_b) = (4.20 \pm 0.07)$ GeV, $\overline{m}_u(2 \text{ GeV}) = 0.0015 \sim 0.003$ GeV,	
$m_e = 0.511 \times 10^{-3}$ GeV, $m_\mu = 0.106$ GeV, $m_\tau = 1.777$ GeV.	[24]
$\tau_{B_s} = (1.437^{+0.030}_{-0.031})$ ps, $\tau_{B_d} = (1.530 \pm 0.009)$ ps, $\tau_{B_u} = (1.638 \pm 0.011)$ ps.	[24]
$f_{B_u} = 0.161 \pm 0.013$ GeV.	[22]
$ V_{ub} = (4.31 \pm 0.39) \times 10^{-3}$.	[25]
$\epsilon_0 \in [-0.01, 0.01]$.	[11]

For the form factors involving the $B \rightarrow P(V)$ transitions, we will use the recent light-cone QCD sum rules (LCSRs) results [22], which are renewed with radiative corrections to the leading twist wave functions and SU(3) breaking effects. For the s -dependence of the form factors, they can be parameterized in terms of simple formulae with two or three parameters. The form factors V^V , A_0^V and f_+^π are parameterized by

$$F(s) = \frac{r_1}{1 - s/m_R^2} + \frac{r_2}{1 - s/m_{fit}^2}. \quad (28)$$

For the form factors A_2^V and f_+^K , it is more appropriate to expand to second order around the pole, yielding

$$F(s) = \frac{r_1}{1 - s/m^2} + \frac{r_2}{(1 - s/m^2)^2}, \quad (29)$$

where $m = m_{fit}$ for A_2^V and $m = m_R$ for f_+^K . The fit formula for A_1^V and f_0^P is

$$F(s) = \frac{r_2}{1 - s/m_{fit}^2}. \quad (30)$$

However, $B_s \rightarrow K$ form factors are not given in LCSR results [22]. After discussions with authors of Ref. [22], we obtain them as

$$F^{B_s \rightarrow K}(s) = F^{B_{u,d} \rightarrow K}(s) \left(\frac{F^{B_s \rightarrow K^*}(s)}{F^{B_{u,d} \rightarrow K^*}(s)} \right). \quad (31)$$

All the corresponding parameters for these form factors are collected in Table II.

We have several remarks on the input parameters:

Table II: Fit for form factors involving the $B \rightarrow K^{(*)}$ and $B \rightarrow \rho(\pi)$ transitions valid for general s [22].

$F(s)$	$F(0)$	r_1	m_R^2	r_2	m_{fit}^2	fit Eq.
$V^{B_{u,d} \rightarrow \rho}$	0.323 ± 0.030	1.045	5.32^2	-0.721	38.34	(28)
$A_0^{B_{u,d} \rightarrow \rho}$	0.303 ± 0.029	1.527	5.28^2	-1.220	33.36	(28)
$A_1^{B_{u,d} \rightarrow \rho}$	0.242 ± 0.023			0.240	37.51	(30)
$A_2^{B_{u,d} \rightarrow \rho}$	0.221 ± 0.023	0.009		0.212	40.82	(29)
$V^{B_{u,d} \rightarrow K^*}$	0.411 ± 0.033	0.923	5.32^2	-0.511	49.40	(28)
$A_0^{B_{u,d} \rightarrow K^*}$	0.374 ± 0.033	1.364	5.28^2	-0.990	36.78	(28)
$A_1^{B_{u,d} \rightarrow K^*}$	0.292 ± 0.028			0.290	40.38	(30)
$A_2^{B_{u,d} \rightarrow K^*}$	0.259 ± 0.027	-0.084		0.342	52.00	(29)
$V^{B_s \rightarrow K^*}$	0.311 ± 0.026	2.351	5.42^2	-2.039	33.10	(28)
$A_0^{B_s \rightarrow K^*}$	0.360 ± 0.034	2.813	5.37^2	-2.509	31.58	(28)
$A_1^{B_s \rightarrow K^*}$	0.233 ± 0.022			0.231	32.94	(30)
$A_2^{B_s \rightarrow K^*}$	0.181 ± 0.025	-0.011		0.192	40.14	(29)
$f_+^{B_{u,d} \rightarrow \pi}$	0.258 ± 0.031	0.744	5.32^2	-0.486	40.73	(28)
$f_0^{B_{u,d} \rightarrow \pi}$	0.258 ± 0.031	0		0.258	33.81	(30)
$f_+^{B_{u,d} \rightarrow K}$	0.331 ± 0.041	0.162	5.41^2	0.173		(29)
$f_0^{B_{u,d} \rightarrow K}$	0.331 ± 0.041	0		0.331	37.46	(30)

- Form factor: The uncertainties of form factors at $s = 0$ induced by $F(0)$ are considered.
- CKM matrix element: Using experimental measurements of $|V_{ub}|$ from the inclusive $b \rightarrow u$ semileptonic B decays, these exclusive $b \rightarrow u \ell^- \bar{\nu}_\ell$ decays can be used to constrain the parameters of theories beyond the SM. The weak phase γ is well constrained in the SM, however, with the presence of R_p violation, this constraint may be relaxed. We will not take γ within the SM range, but vary it randomly in the range of 0 to π to obtain conservative limits on RPV coupling products.
- RPV coupling: When we study the RPV effects, we consider only one RPV coupling product contributes at one time, neglecting the interferences between different RPV coupling

products, but keeping their interferences with the SM amplitude. We assume the masses of sfermion are 100 GeV. For other values of the sfermion masses, the bounds on the couplings in this paper can be easily obtained by scaling them by factor $\tilde{f}^2 \equiv (\frac{m_{\tilde{f}}}{100 \text{ GeV}})^2$.

4 Numerical results in the MSSM with RPC

In this section, we study the charged Higgs contributions to the exclusive $\bar{b} \rightarrow \bar{u}\ell^+\nu_\ell$ decays in the MSSM with RPC. Since the couplings of the charged Higgs to the leptons are always proportional to the charged lepton masses (see the foregoing equations), it is easily to understand that the effects of the charged Higgs will not significantly affect in the case of the light leptonic decays, so we only present the charged Higgs contributions to the exclusive $\bar{b} \rightarrow \bar{u}\tau^+\nu_\tau$ decays. Based on the constraint of the charged Higgs effects from the measurement on $\mathcal{B}(B^+ \rightarrow \tau^+\nu_\tau)$, we investigate these effects on \mathcal{B} , $d\mathcal{B}/ds$, $\overline{\mathcal{A}}_{FB}$ and Γ_L^V/Γ_T^V in the exclusive $\bar{b} \rightarrow \bar{u}\tau^+\nu_\tau$ semileptonic decays.

Note that the charged Higgs effects on the exclusive $\bar{b} \rightarrow \bar{u}\tau^+\nu_\tau$ decays have been discussed in Ref. [26], which fixed $\tan\beta = 50$ and let physical quantity as a function of m_H . Here we will not choose $\tan\beta$ as a fixed value but let observable as a function of $\tan\beta$ and m_H to study the effects of $\tan\beta$ and m_H . In addition, we will investigate the charged Higgs contributions to Γ_L^V/Γ_T^V , which has not been studied yet. For the exclusive $\bar{b} \rightarrow \bar{u}\tau^+\nu_\tau$ decays, the purely leptonic decay $B_u^+ \rightarrow \tau^+\nu_\tau$ has been measured by *BABAR* [27] and *Belle* [28]. We will use the averaged experimental data from Heavy Flavor Averaging Group [25]

$$\mathcal{B}(B_u^+ \rightarrow \tau^+\nu_\tau) = (1.41_{-0.42}^{+0.43}) \times 10^{-4}. \quad (32)$$

Using the experimental data of $\mathcal{B}(B_u^+ \rightarrow \tau^+\nu_\tau)$ varied randomly within 1σ range and considering the theoretical uncertainties, we constrain the allowed range of $\tan\beta/m_H$, which is shown in Fig. 3(a). The corresponding bound from the upper limit of $\mathcal{B}(B_u^+ \rightarrow \mu^+\nu_\mu) < 1.7 \times 10^{-6}$ is also displayed in Fig. 3(b), in which the bound is weaker than one from $\mathcal{B}(B_u^+ \rightarrow \tau^+\nu_\tau)$. At present, the most stringent bound comes from $B_u^+ \rightarrow \tau^+\nu_\tau$. The numerical ranges of $\tan\beta/m_H$ without the radiative corrections ($\epsilon_0 = 0$) and with inclusion of radiative corrections ($\epsilon_0 \in [-0.01, 0.01]$) are given in Table III. In Ref. [29], from the experimental upper limit of $\mathcal{B}(B_u^+ \rightarrow \tau^+\nu_\tau) < 4.1 \times 10^{-4}$, the authors got $\tan\beta/m_H = 0.34(0.36, 0.32) \text{ GeV}^{-1}$

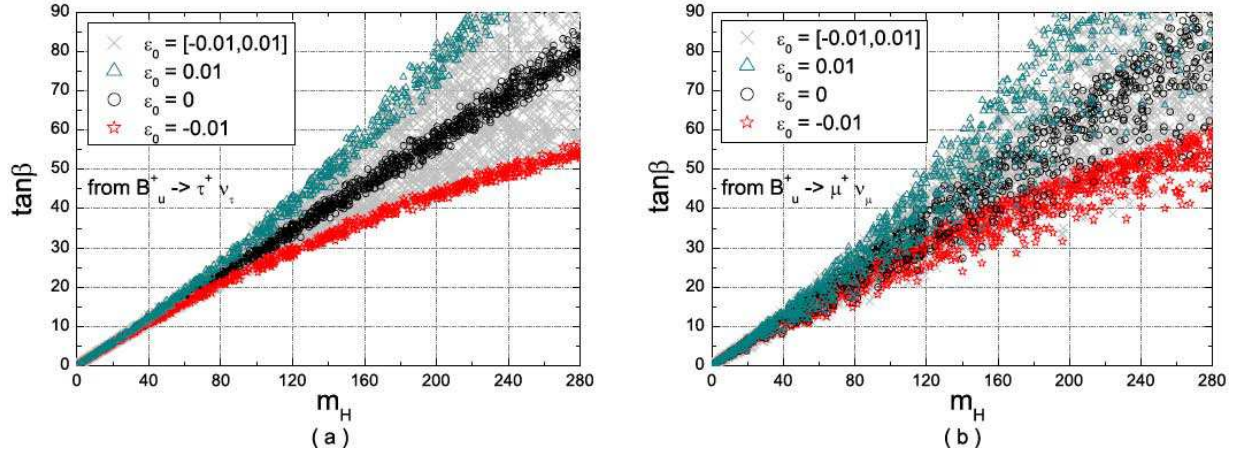


Figure 3: The allowed regions in the $\tan\beta$ - m_H plane for different values of ϵ_0 . Plot (a) is constrained from the experimental data of $\mathcal{B}(B_u^+ \rightarrow \tau^+\nu_\tau)$, and plot (b) is constrained from the upper limit of $\mathcal{B}(B_u^+ \rightarrow \mu^+\nu_\mu)$.

Table III: The allowed ranges of $\tan\beta/m_H$ from $\mathcal{B}(B_u^+ \rightarrow \tau^+\nu_\tau)$ and $\mathcal{B}(B_u^+ \rightarrow \mu^+\nu_\mu)$.

	$\epsilon_0 = 0$	$\epsilon_0 \in [-0.01, 0.01]$
$\tan\beta/m_H$ from $\mathcal{B}(B_u^+ \rightarrow \tau^+\nu_\tau)$	[0.26,0.31] GeV ⁻¹	[0.18,0.49] GeV ⁻¹
$\tan\beta/m_H$ from $\mathcal{B}(B_u^+ \rightarrow \mu^+\nu_\mu)$	[0.20,0.34] GeV ⁻¹	[0.15,0.57] GeV ⁻¹

for $f_{B_u} = 0.2(0.17, 0.23)$ GeV with $\epsilon_0 = 0$. Our bounds on $\tan\beta/m_H$, from new data of $\mathcal{B}(B_u^+ \rightarrow \tau^+\nu_\tau)$ and with considering all theoretical uncertainties, are much stronger than theirs, as shown in Table III.

Using the constrained $\tan\beta/m_H$ from $\mathcal{B}(B_u^+ \rightarrow \tau^+\nu_\tau)$, one can predict the charged Higgs effects on the semileptonic decays $B_u^+ \rightarrow \pi^0\tau^+\nu_\tau$, $B_d^0 \rightarrow \pi^-\tau^+\nu_\tau$, $B_s^0 \rightarrow K^-\tau^+\nu_\tau$, $B_u^+ \rightarrow \rho^0\tau^+\nu_\tau$, $B_d^0 \rightarrow \rho^-\tau^+\nu_\tau$ and $B_s^0 \rightarrow K^{*-}\tau^+\nu_\tau$. With the expressions for \mathcal{B} and Γ_L^V/Γ_T^V at hand, we perform a scan on the input parameters and the newly constrained $\tan\beta/m_H$. Then, the allowed ranges for \mathcal{B} and Γ_L^V/Γ_T^V are obtained including the charged Higgs contributions, which satisfy present experimental constraint of $\mathcal{B}(B_u^+ \rightarrow \tau^+\nu_\tau)$ shown in Eq. (32). Our numerical results are summarized in Table VI, in which we find that the charged Higgs contributions could slightly reduce $\mathcal{B}(B \rightarrow P(V)\tau\nu_\tau)$ and $\frac{\Gamma_L}{\Gamma_T}(B \rightarrow V\tau^+\nu_\tau)$.

Now, we present correlations between the physical observables and the charged Higgs effects by the two-dimensional scatter plots, and moreover, we give the SM predictions for comparison.

Table VI: The theoretical predictions of the exclusive $\bar{b} \rightarrow \bar{u}\tau^+\nu_\tau$ decays for $\mathcal{B}(\times 10^{-4})$ and Γ_L^V/Γ_T^V in the SM and in the MSSM with RPC.

	SM value	MSSM value w/ RPC
$\mathcal{B}(B_u^+ \rightarrow \pi^0\tau^+\nu_\tau)$	[0.58, 1.22]	[0.43, 0.96]
$\mathcal{B}(B_d^0 \rightarrow \pi^-\tau^+\nu_\tau)$	[1.12, 2.28]	[0.80, 1.79]
$\mathcal{B}(B_s^0 \rightarrow K^-\tau^+\nu_\tau)$	[1.47, 3.05]	[1.02, 2.37]
$\mathcal{B}(B_u^+ \rightarrow \rho^0\tau^+\nu_\tau)$	[0.97, 2.19]	[0.83, 2.02]
$\mathcal{B}(B_d^0 \rightarrow \rho^-\tau^+\nu_\tau)$	[1.83, 4.08]	[1.56, 3.78]
$\mathcal{B}(B_s^0 \rightarrow K^{*-}\tau^+\nu_\tau)$	[2.08, 4.46]	[1.64, 4.06]
$\frac{\Gamma_L}{\Gamma_T}(B_u^+ \rightarrow \rho^0\tau^+\nu_\tau)$	[0.65, 1.19]	[0.45, 1.03]
$\frac{\Gamma_L}{\Gamma_T}(B_d^0 \rightarrow \rho^-\tau^+\nu_\tau)$	[0.65, 1.19]	[0.45, 1.03]
$\frac{\Gamma_L}{\Gamma_T}(B_s^0 \rightarrow K^{*-}\tau^+\nu_\tau)$	[0.84, 1.38]	[0.58, 1.11]

The charged Higgs effects on $B_u^+ \rightarrow \pi^0\tau^+\nu_\tau$, $B_d^0 \rightarrow \pi^-\tau^+\nu_\tau$ and $B_s^0 \rightarrow K^-\tau^+\nu_\tau$ are very similar to each other, therefore we will take $B_d^0 \rightarrow \pi^-\tau^+\nu_\tau$ decay as an example. For the same reason, we will only display the charged Higgs effects on $B_d^0 \rightarrow \rho^-\tau^+\nu_\tau$ among other three decay modes $B_u^+ \rightarrow \rho^0\tau^+\nu_\tau$, $B_d^0 \rightarrow \rho^-\tau^+\nu_\tau$ and $B_s^0 \rightarrow K^{*-}\tau^+\nu_\tau$. The charged Higgs effects on $B_d^0 \rightarrow \pi^-(\rho^-\tau^+\nu_\tau)$ decays are shown in Fig. 4.

From Fig. 4(a-c), we can see that $\mathcal{B}(B_d^0 \rightarrow \pi^-\tau^+\nu_\tau)$, $\mathcal{B}(B_d^0 \rightarrow \rho^-\tau^+\nu_\tau)$ and $\frac{\Gamma_L}{\Gamma_T}(B_d^0 \rightarrow \rho^-\tau^+\nu_\tau)$ are not much sensitive to the change of $\tan\beta/m_H$, but the charged Higgs contributions can slightly reduce these quantities. As shown in Fig. 4(d-g), the charged Higgs have also reducing effects on $d\mathcal{B}/ds$ and $\overline{\mathcal{A}}_{FB}$. Especially, the sign of $\overline{\mathcal{A}}_{FB}(B_d^0 \rightarrow \pi^-\tau^+\nu_\tau)$ could be changed by the effect. According to Eqs. (12)-(17), since the normalized FB asymmetry of $B \rightarrow P\ell^+\nu_\ell$ is associated with $m_\ell^2 f_0^P(s)f_+^P(s)$ and not suppressed by s , we can easily understand that $\overline{\mathcal{A}}_{FB}(B_d^0 \rightarrow \pi^-\tau^+\nu_\tau)$ shown in Fig. 4(f) could be significantly affected by the charged Higgs couplings. Therefore, $\overline{\mathcal{A}}_{FB}(B \rightarrow P\tau^+\nu_\tau)$ are very powerful quantities to be measured, to constrain the charged Higgs effects in the MSSM with RPC.

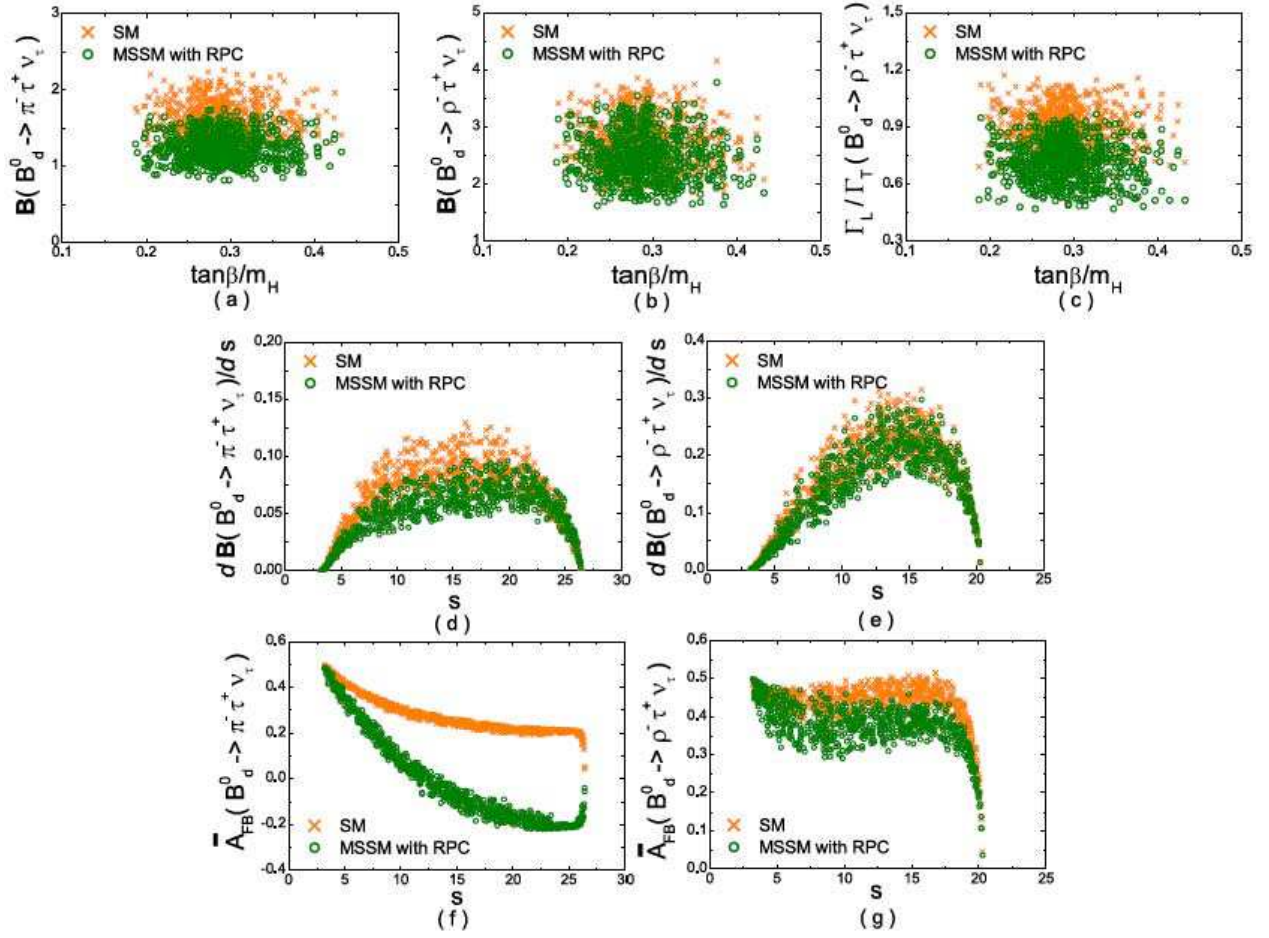


Figure 4: The charged Higgs effects on $B_d^0 \rightarrow \pi^-(\rho^-)\tau^+\nu_\tau$ decays in the MSSM with RPC. \mathcal{B} and $d\mathcal{B}/ds$ are in unit of 10^{-4} .

5 Numerical results in the RPV MSSM

5.1 The exclusive $\bar{b} \rightarrow \bar{u}\tau^+\nu_\tau$ decays

There are two RPV coupling products, $\lambda_{33i}^*\lambda'_{31i}$ and $\lambda_{i33}^*\lambda'_{i13}$, contributing to seven exclusive $\bar{b} \rightarrow \bar{u}\tau^+\nu_\tau$ decay modes, $B_u^+ \rightarrow \tau^+\nu_\tau$, $B_u^+ \rightarrow \pi^0\tau^+\nu_\tau$, $B_d^0 \rightarrow \pi^-\tau^+\nu_\tau$, $B_s^0 \rightarrow K^-\tau^+\nu_\tau$, $B_u^+ \rightarrow \rho^0\tau^+\nu_\tau$, $B_d^0 \rightarrow \rho^-\tau^+\nu_\tau$ and $B_s^0 \rightarrow K^{*-}\tau^+\nu_\tau$. We use the experimental data of $\mathcal{B}(B_u^+ \rightarrow \tau^+\nu_\tau)$, which is varied randomly within 1σ range to constrain the two RPV coupling products. Our bounds on the two RPV coupling products are demonstrated in Fig. 5, in which we find that every RPV weak phase is not much constrained, but the modulus of the relevant RPV coupling products can be tightly upper limited. The upper limits for the relevant RPV coupling products are summarized in Table V. Note that the bounds on the direct quadric couplings have not

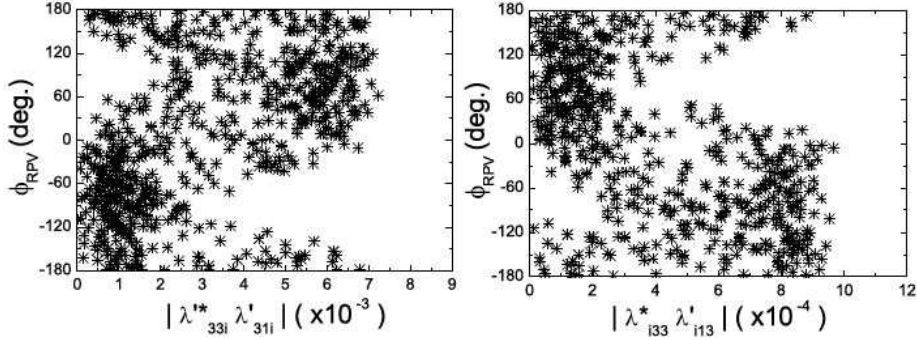


Figure 5: The allowed parameter spaces for the relevant RPV coupling products constrained by the experimental data of $\mathcal{B}(B_u^+ \rightarrow \tau^+ \nu_\tau)$.

Table V: Bounds for the relevant RPV coupling products by $B_u^+ \rightarrow \tau^+ \nu_\tau$ decay for 100 GeV sfermions.

Couplings	Bounds	[Processes]
$ \lambda_{33i}^* \lambda'_{31i} $	$\leq 7.28 \times 10^{-3}$	$[B_u^+ \rightarrow \tau^+ \nu_\tau]$
$ \lambda_{i33}^* \lambda'_{i13} $	$\leq 9.65 \times 10^{-4}$	$[B_u^+ \rightarrow \tau^+ \nu_\tau]$

been estimated in previous $\bar{b} \rightarrow \bar{u} \tau^+ \nu_\tau$ studies. Our bounds on the RPV quadric couplings from $B_u^+ \rightarrow \tau^+ \nu_\tau$ are weaker than the bounds, which are calculated from the products of the smallest values of two single couplings in [30, 31].

Using the constrained parameter spaces shown in Fig. 5, we will predict the RPV effects on other quantities which have not been measured yet in the exclusive $\bar{b} \rightarrow \bar{u} \tau^+ \nu_\tau$ decays. The allowed ranges for \mathcal{B} and Γ_L^V/Γ_T^V are obtained with the different RPV coupling products, which are summarized in Table VI. We can find some salient features of the numerical results listed in Table VI.

- ① The contributions of $\lambda_{33i}^* \lambda'_{31i}$ due to squark exchange will little enhance the branching ratios $\mathcal{B}(B \rightarrow P \tau^+ \nu_\tau)$ and $\mathcal{B}(B \rightarrow V \tau^+ \nu_\tau)$. Because the effective Hamiltonian of squark exchange is proportional to operator $(\bar{b} \gamma_\mu (1 - \gamma_5) u) (\bar{\nu}_\tau \gamma^\mu (1 - \gamma_5) \tau)$, which is the same as the SM one, the effects of squark exchange are completely canceled in $\frac{\Gamma_L}{\Gamma_T}(B \rightarrow V \tau^+ \nu_\tau)$.
- ② As for the contributions of $\lambda_{i33}^* \lambda'_{i13}$ due to slepton exchange, the slepton exchange coupling has not obvious effects on $\mathcal{B}(B \rightarrow P(V) \tau^+ \nu_\tau)$, but the allowed ranges of $\frac{\Gamma_L}{\Gamma_T}(B \rightarrow V \tau^+ \nu_\tau)$

Table VI: The theoretical predictions of the exclusive $\bar{b} \rightarrow \bar{u}\tau^+\nu_\tau$ decays for $\mathcal{B}(\times 10^{-4})$ and Γ_L^V/Γ_T^V in the SM and the RPV MSSM. The RPV MSSM predictions are obtained by the constrained regions of the different RPV coupling products.

	SM value	MSSM value w/ $\lambda_{33i}^*\lambda'_{31i}$	MSSM value w/ $\lambda_{i33}^*\lambda'_{i13}$
$\mathcal{B}(B_u^+ \rightarrow \pi^0\tau^+\nu_\tau)$	[0.58, 1.22]	[0.78, 2.47]	[0.49, 1.30]
$\mathcal{B}(B_d^0 \rightarrow \pi^-\tau^+\nu_\tau)$	[1.12, 2.28]	[1.45, 4.59]	[0.91, 2.41]
$\mathcal{B}(B_s^0 \rightarrow K^-\tau^+\nu_\tau)$	[1.47, 3.05]	[1.92, 5.91]	[1.18, 3.35]
$\mathcal{B}(B_u^+ \rightarrow \rho^0\tau^+\nu_\tau)$	[0.97, 2.19]	[1.42, 4.07]	[0.89, 2.17]
$\mathcal{B}(B_d^0 \rightarrow \rho^-\tau^+\nu_\tau)$	[1.83, 4.08]	[2.64, 7.57]	[1.65, 4.04]
$\mathcal{B}(B_s^0 \rightarrow K^{*-}\tau^+\nu_\tau)$	[2.08, 4.46]	[2.85, 9.62]	[1.96, 4.57]
$\frac{\Gamma_L}{\Gamma_T}(B_u^+ \rightarrow \rho^0\tau^+\nu_\tau)$	[0.65, 1.19]	[0.47, 1.22]
$\frac{\Gamma_L}{\Gamma_T}(B_d^0 \rightarrow \rho^-\tau^+\nu_\tau)$	[0.65, 1.19]	[0.47, 1.22]
$\frac{\Gamma_L}{\Gamma_T}(B_s^0 \rightarrow K^{*-}\tau^+\nu_\tau)$	[0.84, 1.38]	[0.68, 1.41]

can be enlarged by this coupling, especially, their allowed lower limits are observably decreased.

For each RPV coupling product, we can present the correlations of \mathcal{B} and Γ_L^V/Γ_T^V within the constrained parameter space displayed in Fig. 5 by the three-dimensional scatter plots. The differential branching ratio $d\mathcal{B}/ds$ and the normalized FB asymmetry $\bar{\mathcal{A}}_{FB}$ can be shown by the two-dimensional scatter plots. The RPV coupling $\lambda_{33i}^*\lambda'_{31i}$ or $\lambda_{i33}^*\lambda'_{i13}$ contributions to $B_u^+ \rightarrow \pi^0(\rho^0)\tau^+\nu_\tau$, $B_d^0 \rightarrow \pi^-(\rho^-)\tau^+\nu_\tau$ and $B_s^0 \rightarrow K^-(K^{*-})\tau^+\nu_\tau$ are also very similar to each other. So we will take an example for $B_d^0 \rightarrow \pi^-(\rho^-)\tau^+\nu_\tau$ decay to illustrate the RPV coupling effects. The effects of the RPV couplings $\lambda_{33i}^*\lambda'_{31i}$ and $\lambda_{i33}^*\lambda'_{i13}$ on $B_d^0 \rightarrow \pi^-(\rho^-)\tau^+\nu_\tau$ decays are shown in Fig. 6 and Fig. 7, respectively.

Now we turn to discuss plots of Fig. 6 in detail. The three-dimensional scatter plots Figs. 6(a-b) show $\mathcal{B}(B_d^0 \rightarrow \pi^-(\rho^-)\tau^+\nu_\tau)$ correlated with $|\lambda_{33i}^*\lambda'_{31i}|$ and its phase $\phi_{\mathbb{R}_p}$. We also give projections to three perpendicular planes, where the $|\lambda_{33i}^*\lambda'_{31i}|-\phi_{\mathbb{R}_p}$ plane displays the constrained regions of $\lambda_{33i}^*\lambda'_{31i}$, as the first plot of Fig. 5. It's shown that $\mathcal{B}(B_d^0 \rightarrow \pi^-(\rho^-)\tau^+\nu_\tau)$ has some sensitivity to $|\lambda_{33i}^*\lambda'_{31i}|$ on the $\mathcal{B}(B_d^0 \rightarrow \pi^-(\rho^-)\tau^+\nu_\tau)$ - $|\lambda_{33i}^*\lambda'_{31i}|$ plane. However, from the $\mathcal{B}(B_d^0 \rightarrow \pi^-(\rho^-)\tau^+\nu_\tau)$ - $\phi_{\mathbb{R}_p}$ plane, we see that $\mathcal{B}(B_d^0 \rightarrow \pi^-(\rho^-)\tau^+\nu_\tau)$ is very insensitive to

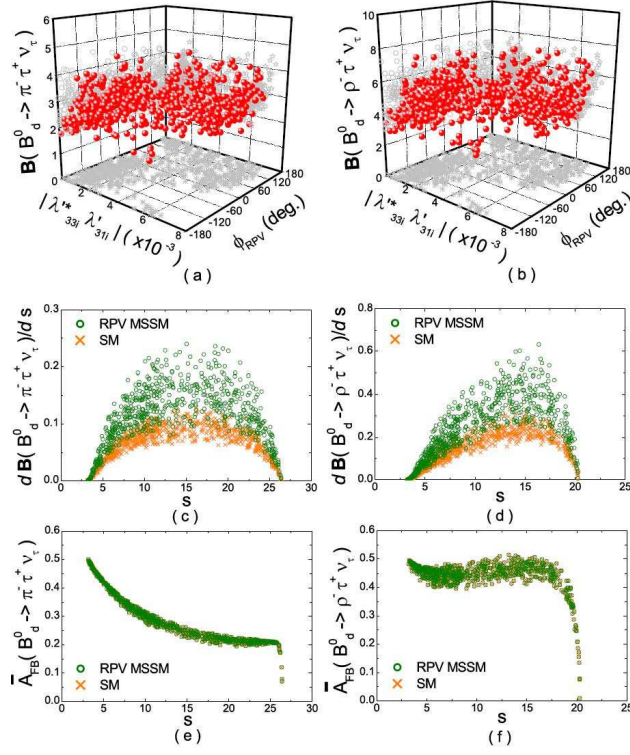


Figure 6: The effects of RPV coupling $\lambda_{33i}^* \lambda'_{31i}$ on $B_d^0 \rightarrow \pi^-(\rho^-)\tau^+\nu_\tau$ decays. \mathcal{B} and $d\mathcal{B}/ds$ are in unit of 10^{-4} .

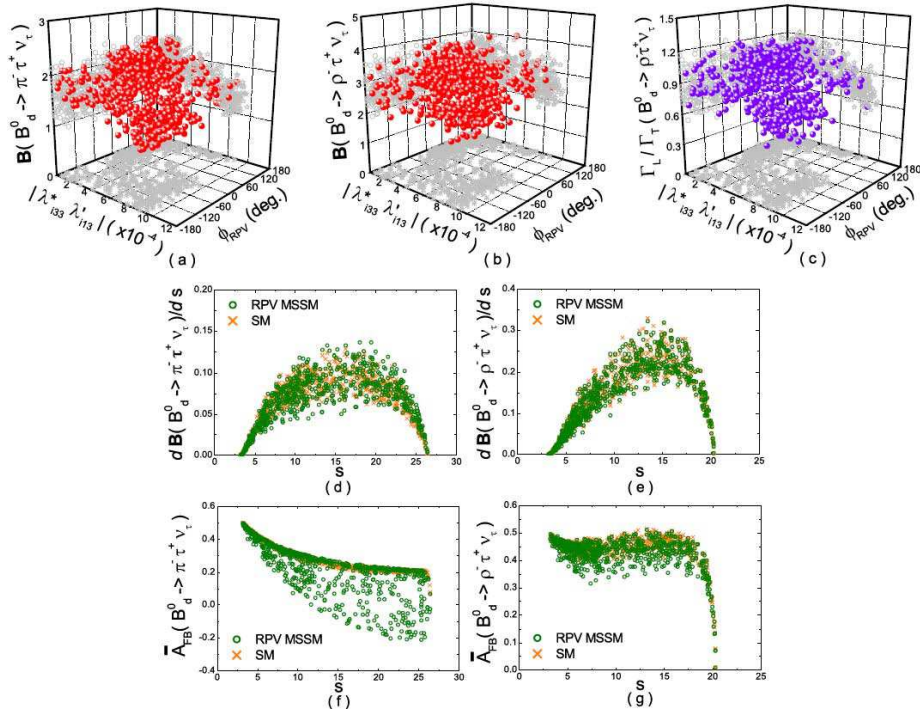


Figure 7: The effects of RPV coupling $\lambda_{i33}^* \lambda'_{i13}$ on $B_d^0 \rightarrow \pi^-(\rho^-)\tau^+\nu_\tau$ decays. \mathcal{B} and $d\mathcal{B}/ds$ are in unit of 10^{-4} .

$|\phi_{R_p}|$. As shown in Fig. 6(e-f), $\overline{\mathcal{A}}_{FB}(B_d^0 \rightarrow \pi^- \tau^+ \nu_\tau)$ and $\overline{\mathcal{A}}_{FB}(B_d^0 \rightarrow \rho^- \tau^+ \nu_\tau)$ are not obviously affected by squark exchange coupling $\lambda_{33i}^* \lambda'_{31i}$, too. In Fig. 6(c-d), the $\lambda_{33i}^* \lambda'_{31i}$ contributions to $d\mathcal{B}(B_d^0 \rightarrow \pi^- (\rho^-) \tau^+ \nu_\tau)/ds$ are possibly distinguishable from the SM expectations at all s regions.

Fig. 7 illustrates the $\lambda_{i33}^* \lambda'_{i13}$ contributions to $B_d^0 \rightarrow \pi^- (\rho^-) \tau^+ \nu_\tau$ decays. $\mathcal{B}(B_d^0 \rightarrow \pi^- \tau^+ \nu_\tau)$, $\mathcal{B}(B_d^0 \rightarrow \rho^- \tau^+ \nu_\tau)$ and $\frac{\Gamma_L}{\Gamma_T}(B_d^0 \rightarrow \rho^- \tau^+ \nu_\tau)$ are all decreasing with $|\lambda_{i33}^* \lambda'_{i13}|$, as shown in Fig. 7(a-c). From Fig. 7(f-g), the effect of $\lambda_{i33}^* \lambda'_{i13}$ could allow that $\overline{\mathcal{A}}_{FB}(B_d^0 \rightarrow \pi^- \tau^+ \nu_\tau)$ and $\overline{\mathcal{A}}_{FB}(B_d^0 \rightarrow \rho^- \tau^+ \nu_\tau)$ have smaller values and, especially, the sign of $\overline{\mathcal{A}}_{FB}(B_d^0 \rightarrow \pi^- \tau^+ \nu_\tau)$ could be changed by the effect. There is similar reason for significant effects of slepton exchange on $\overline{\mathcal{A}}_{FB}(B \rightarrow P \tau^+ \nu_\tau)$ as Fig. 4(f), *i.e.* the normalized FB asymmetry is not suppressed by m_ℓ^2 and s . The different effects between the charged Higgs and slepton exchange on $\overline{\mathcal{A}}_{FB}(B \rightarrow P \tau^+ \nu_\tau)$, shown in Fig. 4(f) and Fig. 7(f), come from the RPV weak phase ϕ_{R_p} and the CKM weak phase γ . The weak phases contribute only to the RPV MSSM predictions of $\overline{\mathcal{A}}_{FB}(B \rightarrow P \tau^+ \nu_\tau)$.

5.2 The exclusive $b \rightarrow u \ell' \nu_{\ell'}$ ($\ell' = \mu$ or e) decays

For the exclusive $b \rightarrow u \ell' \nu_{\ell'}$ decays, several branching ratios have been accurately measured by *BABAR*, Belle and CLEO [32, 33, 34, 35, 36, 37]. Their averaged values from PDG [24] and corresponding SM prediction values are given in Table VII. The experimental results are roughly consistent with the SM predictions, nevertheless there are still windows for NP in these

Table VII: The experimental data for the exclusive $\bar{b} \rightarrow \bar{u} \ell'^+ \nu_{\ell'}$ decays [24, 32, 33, 34, 35, 36, 37] and corresponding SM predictions.

	Experimental data	SM value for $\ell' = \mu$	SM value for $\ell' = e$
$\mathcal{B}(B_u^+ \rightarrow \mu^+ \nu_\mu)$	$< 1.7 \times 10^{-6}$ 90% C.L.	$[2.69, 5.30] \times 10^{-7}$	
$\mathcal{B}(B_u^+ \rightarrow e^+ \nu_e)$	$< 9.8 \times 10^{-7}$ 90% C.L.		$[6.28, 12.46] \times 10^{-12}$
$\mathcal{B}(B_u^+ \rightarrow \pi^0 \ell'^+ \nu_{\ell'})$	$(0.75 \pm 0.09) \times 10^{-4}$	$[0.76, 1.75] \times 10^{-4}$	$[0.75, 1.75] \times 10^{-4}$
$\mathcal{B}(B_d^0 \rightarrow \pi^- \ell'^+ \nu_{\ell'})$	$(1.41 \pm 0.08) \times 10^{-4}$	$[1.41, 3.25] \times 10^{-4}$	$[1.40, 3.27] \times 10^{-4}$
$\mathcal{B}(B_u^+ \rightarrow \rho^0 \ell'^+ \nu_{\ell'})$	$(1.28 \pm 0.18) \times 10^{-4}$	$[1.49, 4.32] \times 10^{-4}$	$[1.48, 4.45] \times 10^{-4}$
$\mathcal{B}(B_d^0 \rightarrow \rho^- \ell'^+ \nu_{\ell'})$	$(2.2 \pm 0.4) \times 10^{-4}$	$[2.78, 8.02] \times 10^{-4}$	$[2.77, 8.32] \times 10^{-4}$

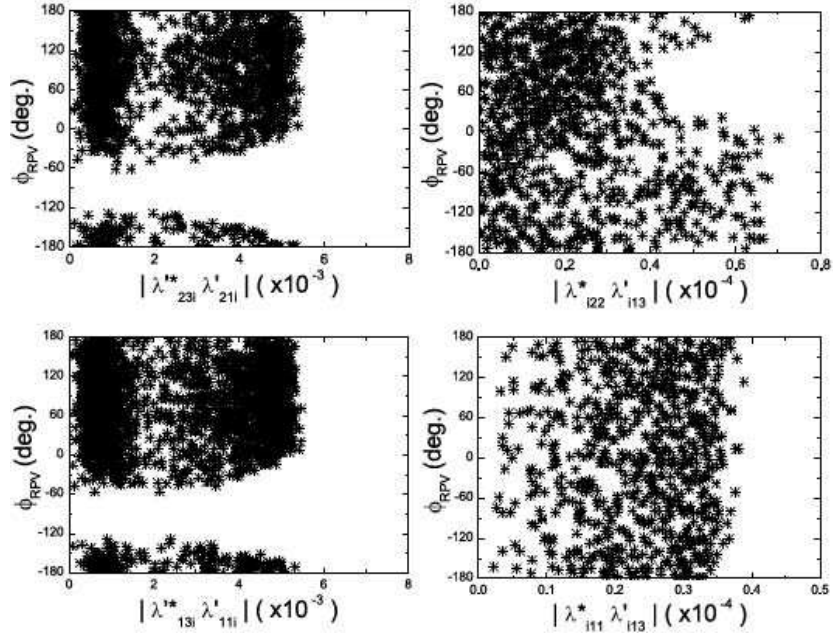


Figure 8: The allowed parameter spaces for the relevant RPV coupling products constrained by the measurements of the exclusive $\bar{b} \rightarrow \bar{u}\ell^+\nu_{\ell'}$ decays listed in Table VII.

processes. Because many branching ratios have been accurately measured, in order to easily obtain the solution of the RPV coupling products, we will use the experimental data given in Table VII, which are varied randomly within 2σ range to constrain the RPV coupling products.

Four RPV coupling products $\lambda_{23i}^* \lambda'_{21i}$, $\lambda_{i22}^* \lambda'_{i13}$ for $\ell' = \mu$ and $\lambda_{13i}^* \lambda'_{11i}$, $\lambda_{i11}^* \lambda'_{i13}$ for $\ell' = e$ are related to fourteen exclusive $b \rightarrow u\ell^+\nu_{\ell'}$ decay modes. We use $\mathcal{B}(B_u^+ \rightarrow \ell^+\nu_{\ell'})$, $\mathcal{B}(B_d^0 \rightarrow \pi^-(\rho^-)\ell^+\nu_{\ell'})$, $\mathcal{B}(B_u^+ \rightarrow \pi^+(\rho^+)\ell^+\nu_{\ell'})$ and their experimental data listed in Table VII to restrict the relevant RPV parameter spaces. The random variation of the parameters subjected to the constraints as discussed above leads to the scatter plots displayed in Fig. 8. In Fig. 8, the RPV weak phases of the slepton exchange couplings $\lambda_{i22}^* \lambda'_{i13}$ and $\lambda_{i11}^* \lambda'_{i13}$ have the entirely allowed ranges $[-180^\circ, 180^\circ]$, but for every RPV weak phase of the squark exchange couplings $\lambda_{23i}^* \lambda'_{21i}$ and $\lambda_{13i}^* \lambda'_{11i}$, there are two possible bands. For $\lambda_{23i}^* \lambda'_{21i}$, one band of its phase is $\phi_{R_p} \in [-180^\circ, -129^\circ]$, another is $\phi_{R_p} \in [-61^\circ, 180^\circ]$. And for $\lambda_{13i}^* \lambda'_{11i}$, one band is $\phi_{R_p} \in [-180^\circ, -129^\circ]$, another is $\phi_{R_p} \in [-56^\circ, 180^\circ]$. The magnitudes of the squark and slepton exchange couplings have been upper limited. The upper limits are summarized in Table VIII. Compared with the existing bounds [30, 31, 38], which are estimated from the products of the smallest values of two single couplings, we get quite strong quadric bounds on $|\lambda_{i22}^* \lambda'_{i13}|$ and $|\lambda_{i11}^* \lambda'_{i13}|$, due to the slepton exchange couplings.

Table VIII: Bounds for the relevant RPV coupling products by the exclusive $\bar{b} \rightarrow \bar{u}\ell'^+\nu_{\ell'}$ decays for 100 GeV sfermions, and previous bounds are listed for comparison [30, 31, 38].

Couplings	Bounds	[Processes]	Previous bounds
$ \lambda_{23i}^* \lambda'_{21i} $	$\leq 5.44 \times 10^{-3}$	$[B_u^+ \rightarrow \mu^+ \nu_\mu]_{B \rightarrow M' \mu^+ \nu_\mu}$	$\leq 2.64 \times 10^{-3}$
$ \lambda_{i22}^* \lambda'_{i13} $	$\leq 7.00 \times 10^{-5}$	$[B_u^+ \rightarrow \mu^+ \nu_\mu]_{B \rightarrow M' \mu^+ \nu_\mu}$	$\leq 3.24 \times 10^{-3}$
$ \lambda_{13i}^* \lambda'_{11i} $	$\leq 5.49 \times 10^{-3}$	$[B_u^+ \rightarrow e^+ \nu_e]_{B \rightarrow M' e^+ \nu_e}$	$\leq 5.4 \times 10^{-3}$
$ \lambda_{i11}^* \lambda'_{i13} $	$\leq 3.88 \times 10^{-5}$	$[B_u^+ \rightarrow e^+ \nu_e]_{B \rightarrow M' e^+ \nu_e}$	$\leq 2.89 \times 10^{-3}$ ($i=2$) $\leq 6.82 \times 10^{-3}$ ($i=3$)

Using the constrained parameter spaces shown in Fig. 8, we predict the RPV effects on other quantities which have not been measured yet in the exclusive $\bar{b} \rightarrow \bar{u}\ell'^+\nu_{\ell'}$ decays. Our predictively numerical results are summarized in Table IX. Because the RPV effects on the

Table IX: The theoretical predictions for CP averaged \mathcal{B} and Γ_L^V/Γ_T^V of the exclusive $\bar{b} \rightarrow \bar{u}\ell'^+\nu_{\ell'}$ decays in the SM and the RPV MSSM. The RPV MSSM predictions are obtained by the constrained regions of the different RPV coupling products. The index $g = 1$ and 2 for $\ell' = e$ and μ , respectively.

	SM value	MSSM value w/ $\lambda_{g3i}^* \lambda'_{g1i}$	MSSM value w/ $\lambda_{igg}^* \lambda'_{i13}$
$\mathcal{B}(B_u^+ \rightarrow \mu^+ \nu_\mu)$	$[2.69, 5.30] \times 10^{-7}$	$[1.55, 3.64] \times 10^{-7}$	$[0.03, 16.98] \times 10^{-7}$
$\mathcal{B}(B_s^0 \rightarrow K^- \mu^+ \nu_\mu)$	$[1.98, 4.81] \times 10^{-4}$	$[1.14, 3.07] \times 10^{-4}$	$[2.00, 3.45] \times 10^{-4}$
$\mathcal{B}(B_s^0 \rightarrow K^{*-} \mu^+ \nu_\mu)$	$[3.17, 8.99] \times 10^{-4}$	$[1.99, 5.14] \times 10^{-4}$	$[3.17, 6.43] \times 10^{-4}$
$\frac{\Gamma_L}{\Gamma_T}(B_u^+ \rightarrow \rho^0 \mu^+ \nu_\mu)$	$[0.49, 1.52]$	$[0.54, 0.66]$
$\frac{\Gamma_L}{\Gamma_T}(B_d^0 \rightarrow \rho^+ \mu^+ \nu_\mu)$	$[0.49, 1.52]$	$[0.54, 0.66]$
$\frac{\Gamma_L}{\Gamma_T}(B_s^0 \rightarrow K^{*-} \mu^+ \nu_\mu)$	$[0.68, 1.70]$	$[0.71, 1.63]$
$\mathcal{B}(B_u^+ \rightarrow e^+ \nu_e)$	$[6.26, 12.37] \times 10^{-12}$	$[3.49, 8.60] \times 10^{-12}$	$[6.26 \times 10^{-12}, 9.8 \times 10^{-7}]$
$\mathcal{B}(B_s^0 \rightarrow K^- e^+ \nu_e)$	$[1.99, 4.78] \times 10^{-4}$	$[1.15, 3.07] \times 10^{-4}$	$[2.01, 3.43] \times 10^{-4}$
$\mathcal{B}(B_s^0 \rightarrow K^{*-} e^+ \nu_e)$	$[3.19, 8.96] \times 10^{-4}$	$[1.89, 5.22] \times 10^{-4}$	$[3.29, 6.41] \times 10^{-4}$
$\frac{\Gamma_L}{\Gamma_T}(B_u^+ \rightarrow \rho^0 e^+ \nu_e)$	$[0.48, 1.53]$	$[0.53, 0.66]$
$\frac{\Gamma_L}{\Gamma_T}(B_d^0 \rightarrow \rho^+ e^+ \nu_e)$	$[0.48, 1.53]$	$[0.53, 0.66]$
$\frac{\Gamma_L}{\Gamma_T}(B_s^0 \rightarrow K^{*-} e^+ \nu_e)$	$[0.69, 1.68]$	$[0.73, 1.67]$

exclusive $\bar{b} \rightarrow \bar{u}\mu^+\nu_\mu$ and $\bar{b} \rightarrow \bar{u}e^+\nu_e$ are quite similar, as shown in Table IX, here we give their remarks altogether:

- ① For the squark exchange couplings $\lambda_{g3i}^*\lambda'_{g1i}$, their effects can decrease the upper limits and lower limits of $\mathcal{B}(B_u^+ \rightarrow \ell'^+\nu_{\ell'})$, $\mathcal{B}(B_s^0 \rightarrow K^-\ell'^+\nu_{\ell'})$ and $\mathcal{B}(B_s^0 \rightarrow K^{*-}\ell'^+\nu_{\ell'})$, as well as shrink the allowed ranges of these branching ratios. The squark exchange effects are completely canceled in $\frac{\Gamma_L}{\Gamma_T}(B \rightarrow V\ell'^+\nu_{\ell'})$.
- ② The slepton exchange couplings $\lambda_{igg}^*\lambda'_{i13}$, which satisfy all present experimental constraints, could significantly change the purely leptonic decay branching ratios $\mathcal{B}(B_u^+ \rightarrow \ell'^+\nu_{\ell'})$: They could enhance the ratios to their experimental upper limits. $\mathcal{B}(B_u^+ \rightarrow \mu^+\nu_\mu)$ could be suppressed to 10^{-9} or enhanced to order of 10^{-6} , and $\mathcal{B}(B_u^+ \rightarrow e^+\nu_e)$ could be enhanced 5 orders from order of 10^{-12} to order of 10^{-7} . The reason of these significant effects on $\mathcal{B}(B_u^+ \rightarrow \ell'^+\nu_{\ell'})$ is that the SM effective Hamiltonian is proportional to $(\bar{b}\gamma_\mu(1-\gamma_5)u)(\bar{\nu}_{\ell'}\gamma^\mu(1-\gamma_5)\ell')$, whose contribution to $\mathcal{B}(B_u^+ \rightarrow \ell'^+\nu_{\ell'})$ is suppressed by $m_{\ell'}^2$ due to helicity suppression, while the effective Hamiltonian of slepton exchange is proportional to $(\bar{b}(1-\gamma_5)u)(\bar{\nu}_{\ell'}(1+\gamma_5)\ell')$, whose contribution is not suppressed by $m_{\ell'}^2$. Therefore, compared with the SM contribution, the slepton exchange couplings have great effects on $\mathcal{B}(B_u^+ \rightarrow \ell'^+\nu_{\ell'})$. The allowed ranges of $\mathcal{B}(B_s^0 \rightarrow K^-(K^{*-})\ell'^+\nu_{\ell'})$ and $\frac{\Gamma_L}{\Gamma_T}(B \rightarrow V\ell'^+\nu_{\ell'})$ are shrunken by $\lambda_{igg}^*\lambda'_{i13}$ couplings.

Figs. 9-10 show the RPV contributions in the $\bar{b} \rightarrow \bar{u}\mu^+\nu_\mu$ decays. We view that the trends in the changes of the physical observables with the modulus and weak phase $\phi_{\mathcal{R}_p}$ of the RPV couplings by the three-dimensional scatter plots, and we also compare the SM predictions with the RPV MSSM predictions in $d\mathcal{B}/ds$ and $\overline{\mathcal{A}}_{FB}$ by the two-dimensional scatter plots. Fig. 9 displays the $\lambda_{23i}^*\lambda'_{21i}$ effects due to the squark exchange couplings on the exclusive $\bar{b} \rightarrow \bar{u}\mu^+\nu_\mu$ decays. From Fig. 9(d-e), we find the contributions of $\lambda_{23i}^*\lambda'_{21i}$ can suppress $d\mathcal{B}(B_s^0 \rightarrow K^-\mu^+\nu_\mu)/ds$ and $d\mathcal{B}(B_s^0 \rightarrow K^{*-}\mu^+\nu_\mu)/ds$, so their contributions are easily distinguishable from the SM predictions with theoretical uncertainties included. However, these contributions to other observables are small, and we cannot find visible effects on $\mathcal{B}(B_u^+ \rightarrow \mu^+\nu_\mu)$, $\mathcal{B}(B_s^0 \rightarrow K^-\mu^+\nu_\mu)$, $\mathcal{B}(B_s^0 \rightarrow K^{*-}\mu^+\nu_\mu)$, $\overline{\mathcal{A}}_{FB}(B_s^0 \rightarrow K^-\mu^+\nu_\mu)$ and $\overline{\mathcal{A}}_{FB}(B_s^0 \rightarrow K^{*-}\mu^+\nu_\mu)$. Fig. 10 presents the $\lambda_{i22}^*\lambda'_{i13}$ effects due to the slepton exchange couplings on the exclusive $\bar{b} \rightarrow \bar{u}\mu^+\nu_\mu$

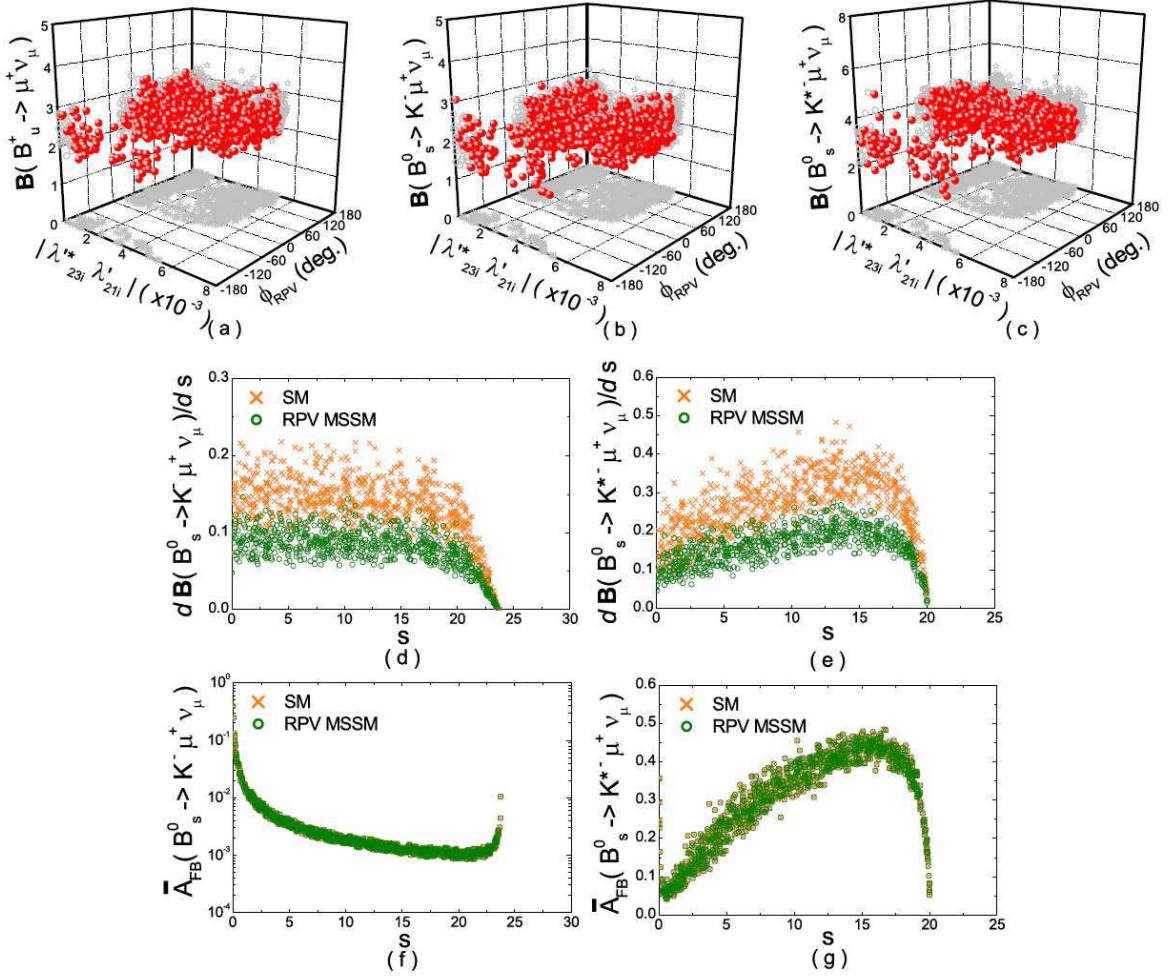


Figure 9: The effects of RPV coupling $\lambda_{23i}^* \lambda'_{21i}$ on the exclusive $\bar{b} \rightarrow \bar{u} \mu^+ \nu_\mu$ decays. \mathcal{B} and $d\mathcal{B}/ds$ of the semileptonic decays are in unit of 10^{-4} , and $\mathcal{B}(B_u^+ \rightarrow \mu^+ \nu_\mu)$ is in unit of 10^{-7} .

decays. The three-dimensional scatter plot Fig. 10(a) shows $\mathcal{B}(B_u^+ \rightarrow \mu^+ \nu_\mu)$ correlated with $|\lambda_{i22}^* \lambda'_{i13}|$ and its phase ϕ_{R_p} , so we can see that $\mathcal{B}(B_u^+ \rightarrow \mu^+ \nu_\mu)$ is greatly increased with $|\lambda_{i22}^* \lambda'_{i13}|$, but is insensitive to ϕ_{R_p} . From Fig. 10(i), we find $\lambda_{i22}^* \lambda'_{i13}$ coupling contributions to $\bar{\mathcal{A}}_{FB}(B_s^0 \rightarrow K^- \mu^+ \nu_\mu)$ are possibly large. There are not obvious $\lambda_{i22}^* \lambda'_{i13}$ coupling effects, overlapping with the SM results in $\mathcal{B}(B_s^0 \rightarrow K^- \mu^+ \nu_\mu)$, $\mathcal{B}(B_s^0 \rightarrow K^{*-} \mu^+ \nu_\mu)$, $\frac{\Gamma_L}{\Gamma_T}(B \rightarrow V \mu^+ \nu_\mu)$, $d\mathcal{B}(B_s^0 \rightarrow K^- \mu^+ \nu_\mu)/ds$, $d\mathcal{B}(B_s^0 \rightarrow K^{*-} \mu^+ \nu_\mu)/ds$ and $\bar{\mathcal{A}}_{FB}(B_s^0 \rightarrow K^{*-} \mu^+ \nu_\mu)$.

For the exclusive $\bar{b} \rightarrow \bar{u} e^+ \nu_e$ decays, the effects of $\lambda_{i11}^* \lambda'_{i13}$ on $\bar{\mathcal{A}}_{FB}(B_s^0 \rightarrow K^- e^+ \nu_e)$ can be distinguishable from the SM prediction, but both the SM prediction and the RPV MSSM prediction are too small to be accessible at LHC.

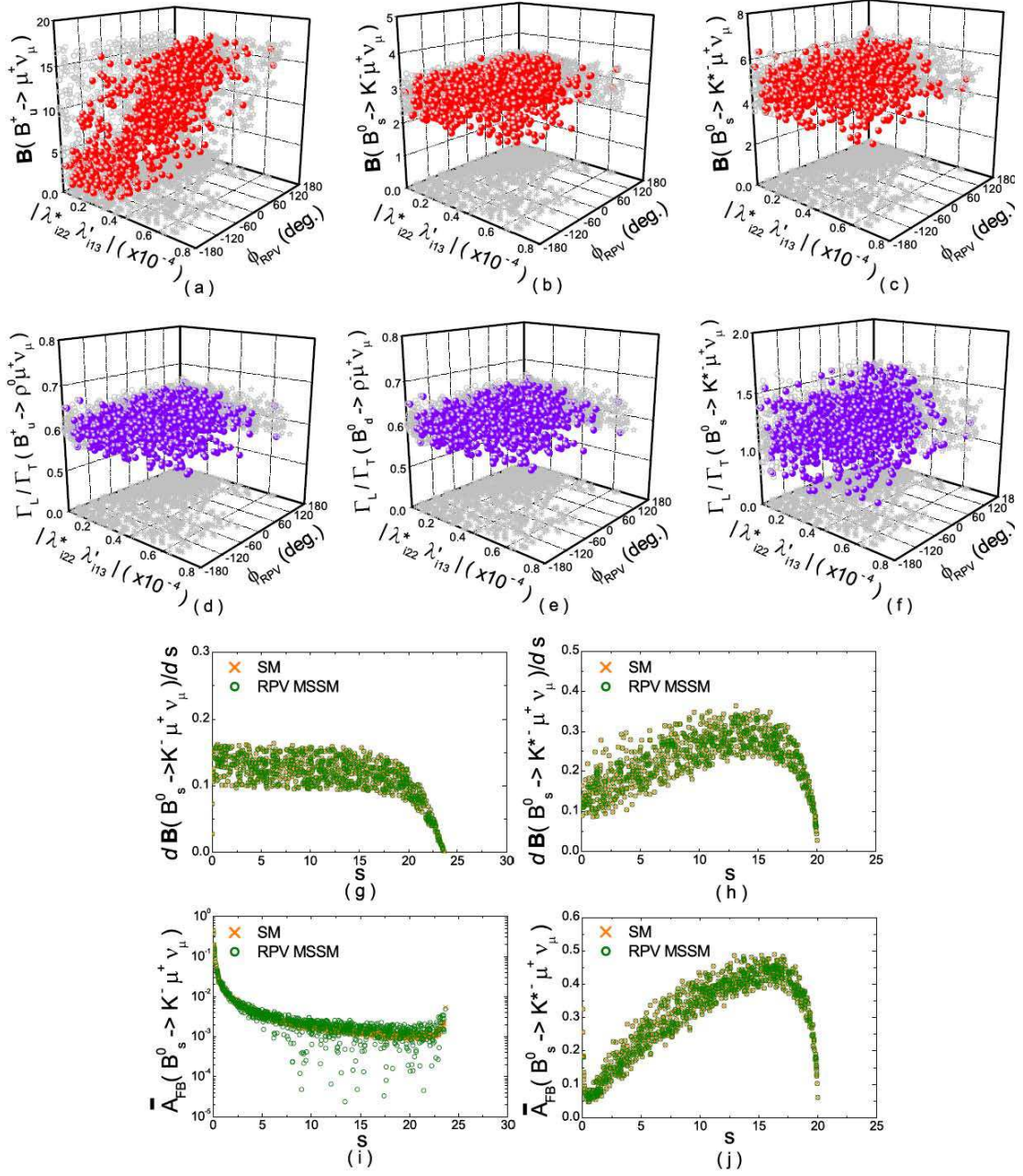


Figure 10: The effects of RPV coupling $\lambda_{i22}^* \lambda'_{i13}$ on the exclusive $\bar{b} \rightarrow \bar{u} \mu^+ \nu_\mu$ decays. \mathcal{B} and $d\mathcal{B}/ds$ of the semileptonic decays are in unit of 10^{-4} , and $\mathcal{B}(B_u^+ \rightarrow \mu^+ \nu_\mu)$ is in unit of 10^{-7} .

6 Summary

In this paper, we have studied the 21 decay channels $B_u^+ \rightarrow \ell^+ \nu_\ell$, $B_u^+ \rightarrow \pi^0 \ell^+ \nu_\ell$, $B_d^0 \rightarrow \pi^- \ell^+ \nu_\ell$, $B_s^0 \rightarrow K^- \ell^+ \nu_\ell$, $B_u^+ \rightarrow \rho^0 \ell^+ \nu_\ell$, $B_d^0 \rightarrow \rho^- \ell^+ \nu_\ell$ and $B_s^0 \rightarrow K^{*-} \ell^+ \nu_\ell$ ($\ell = \tau, \mu, e$) in the MSSM with and without R_p violation. Considering the theoretical uncertainties and the experimental errors, we have obtained fairly constrained parameter spaces of new physics coupling constants

from the present experimental data. Furthermore, we have predicted the charged Higgs effects and the RPV effects on the branching ratios, the normalized FB asymmetries of charged leptons and the ratios of longitudinal to transverse polarization of the vector mesons, which have not been measured or have not been well measured yet.

We have found that both the charged Higgs coupling and the slepton exchange coupling $\lambda_{i33}^* \lambda'_{i13}$ have significant effects on $\overline{\mathcal{A}}_{FB}(B \rightarrow P\tau^+\nu_\tau)$, and the sign of $\overline{\mathcal{A}}_{FB}(B \rightarrow P\tau^+\nu_\tau)$ could be changed by these effects. The charged Higgs effects and the slepton exchange coupling effects are distinguishable in the purely leptonic $B_u^+ \rightarrow \mu^+\nu_\mu, e^+\nu_e$ decays. The charged Higgs coupling has negligible effects on $\mathcal{B}(B_u^+ \rightarrow \mu^+\nu_\mu)$ and $\mathcal{B}(B_u^+ \rightarrow e^+\nu_e)$, but the slepton exchange contributions of the RPV MSSM are very sensitive to $\mathcal{B}(B_u^+ \rightarrow \mu^+\nu_\mu)$ and $\mathcal{B}(B_u^+ \rightarrow e^+\nu_e)$. If the enhancement of branching ratios is not discovered in $B^+ \rightarrow \mu^+\nu_\mu, e^+\nu_e$ decays, the new limits from future experiments would constrain the slepton exchange couplings. Otherwise, it would imply that RPV effects is likely to be seen. We have also compared the SM predictions with the RPV predictions of $d\mathcal{B}/ds$ and $\overline{\mathcal{A}}_{FB}$ in $B \rightarrow P(V)\ell^+\nu_\ell$ decays. We have found that the RPV couplings due to squark exchange are in principle distinguishable from the SM contributions at all kinematic regions in all eighteen semileptonic $d\mathcal{B}/ds$. The results in this paper could be useful for probing the charged Higgs effects and the RPV MSSM effects, and will correlate strongly with searches for the direct SUSY signals at future experiments, for example, LHC and Super- B Factories.

Acknowledgments

We would like to thank Dr. R. Zwicky for useful discussions on $B_s \rightarrow K$ form factors. The work of C.S.K. was supported in part by CHEP-SRC and in part by the KRF Grant funded by the Korean Government (MOEHRD) No. KRF-2005-070-C00030. The work of Ru-Min Wang was supported by the KRF Grant funded by the Korean Government (MOEHRD) No. KRF-2005-070-C00030.

References

- [1] J. F. Gunion, H. E. Haber, G. L. Kane and S. Dawson, “The Higgs Hunters Guide”, Addison-Wesley, Menlo-Park (1990); see also: (E) SCIPP-92-58, hep-ph/9302272.
- [2] P. Fayet, Nucl. Phys. **B90**, 104(1975); Phys. Lett. **B64**, 159(1976); Phys. Lett. **B69**, 489(1977); Phys. Lett. **B84**, 416(1979).
- [3] K. Inoue, A. Komatsu and S. Takeshita, Prog. Theor. Phys. **68**, 927(1982); (E) *ibid.* **70**, 330(1983); H. Nilles, Phys. Rept. **110**, 1(1984); H. Haber and G. Kane, Phys. Rept. **117**, 75(1985).
- [4] Y. Grossman and Z. Ligeti, Phys. Lett. **B332**, 373(1994) [arXiv:hep-ph/9403376]; K. S. Babu and C. Kolda, Phys. Rev. Lett. **84**, 228(2000) [arXiv:hep-ph/9909476].
- [5] C. S. Huang, W. Liao and Q. S. Yan, Phys. Rev. **D59**, 011701(1999) [arXiv:hep-ph/9803460]; C. S. Huang, L. Wei, Q. S. Yan and S. H. Zhu, Phys. Rev. **D63**, 114021(2001), (E) *ibid.* **D64**, 059902(2001) [arXiv:hep-ph/0006250].
- [6] P. H. Chankowski and L. Ślawniowska, Phys. Rev. **D63**, 054012(2001) [arXiv:hep-ph/0008046]; C. Bobeth, T. Ewerth, F. Krüger and J. Urban, Phys. Rev. **D64**, 074014(2001) [arXiv:hep-ph/0104284].
- [7] G. D’Ambrosio, G. F. Giudice, G. Isidori and A. Strumia, Nucl. Phys. **B645**, 155(2002) [arXiv:hep-ph/0207036]; A. J. Buras, P. H. Chankowski, J. Rosiek and L. Ślawniowska, Phys. Lett. **B546**, 96(2002) [arXiv:hep-ph/0207241]; G. Isidori and A. Retico, JHEP **0209**, 063(2002) [arXiv:hep-ph/0208159].
- [8] C. Bobeth, T. Ewerth, F. Krüger and J. Urban, Phys. Rev. **D66**, 074021(2002) [arXiv:hep-ph/0204225]; T. Ibrahim and P. Nath, Phys. Rev. **D67**, 016005(2003) [arXiv:hep-ph/0208142].
- [9] F. Borzumati, C. Greub and Y. Yamada, Phys. Rev. **D69**, 055005(2004) [arXiv:hep-ph/0311151]; S. Baek, Phys. Lett. **B595**, 461(2004) [arXiv:hep-ph/0406007].

- [10] M. S. Carena, A. Menon, R. Noriega-Papaqui, A. Szyrkman and C. E. M. Wagner, Phys. Rev. **D74**, 015009(2006) [arXiv:hep-ph/0603106]; E. Lunghi, W. Porod and O. Vives, Phys. Rev. **D74**, 075003(2006) [arXiv:hep-ph/0605177]; J. Ellis, S. Heinemeyer, K. A. Olive, A. M. Weber and G. Weiglein, JHEP **0708**, 083(2007) [arXiv:0706.0652 [hep-ph]].
- [11] A. J. Buras, P. H. Chankowski, J. Rosiek and L. Ślawniowska, Nucl. Phys. **B659**, 3(2003) [arXiv:hep-ph/0210145].
- [12] W. S. Hou, Phys. Rev. **D48**, 2342(1993); G. Isidori and P. Paradisi, Phys. Lett. **B639**, 499(2006) [arXiv:hep-ph/0605012].
- [13] G. R. Farrar and P. Fayet, Phys. Lett. **B76**, 575(1978).
- [14] J. H. Jang, Y. G. Kim and J. S. Lee, Phys. Lett. **B408**, 367(1997) [arXiv:hep-ph/9704213]; J. H. Jang, Y. G. Kim and J. S. Lee, Phys. Rev. **D58**, 035006(1998) [arXiv:hep-ph/9711504]; G. Bhattacharyya and A. Raychaudhuri, Phys. Rev. **D57**, R3837(1998) [arXiv:hep-ph/9712245].
- [15] G. Bhattacharyya and A. Datta, Phys. Rev. Lett. **83**, 2300(1999) [arXiv:hep-ph/9903490]; D. Chakraverty and D. Choudhury, Phys. Rev. **D63**, 075009(2001) [arXiv:hep-ph/0008165]; B. Dutta, C. S. Kim and S. Oh, Phys. Lett. **B535**, 249(2002) [arXiv:hep-ph/0202019].
- [16] A. Datta, Phys. Rev. **D66**, 071702(2002) [arXiv:hep-ph/0208016]; B. Dutta, C. S. Kim and S. Oh, Phys. Rev. Lett. **90**, 011801(2003) [arXiv:hep-ph/0208226]; J. P. Saha and A. Kundu, Phys. Rev. **D66**, 054021(2002) [arXiv:hep-ph/0205046].
- [17] B. Dutta, C. S. Kim, S. Oh and G. h. Zhu, Eur. Phys. J. **C37**, 273(2004) [arXiv:hep-ph/0312388]; B. Dutta, C. S. Kim, S. Oh and G. h. Zhu, Phys. Lett. **B601**, 144(2004) [arXiv:hep-ph/0312389]; Y. D. Yang, R. M. Wang and G. R. Lu, Phys. Rev. **D72**, 015009(2005) [arXiv:hep-ph/0411211].
- [18] R. Wang, G. R. Lu, E. K. Wang and Y. D. Yang, Eur. Phys. J. **C47**, 815 (2006) [arXiv:hep-ph/0603088]; S. Nandi and J. P. Saha, Phys. Rev. **D74**, 095007(2006)

- [arXiv:hep-ph/0608341]; Y. G. Xu, R. M. Wang and Y. D. Yang, Phys. Rev. **D74**, 114019(2006) [arXiv:hep-ph/0610338].
- [19] H. K. Dreiner, M. Krämer and B. O'leary, Phys. Rev. **D75**, 114016(2007) [arXiv:hep-ph/0612278]; A. Mir and F. Tahir, [arXiv:0707.2268 [hep-ph]]; J. J. Wang, R. M. Wang, Y. G. Xu and Y. D. Yang, [arXiv:0711.0321 [hep-ph]].
- [20] S. Baek and Y. G. Kim, Phys. Rev. **D60**, 077701(1999) [arXiv:hep-ph/9906385]; H. Dreiner, G. Polesello and M. Thormeier, Phys. Rev. **D65**, 115006(2002) [arXiv:hep-ph/0112228].
- [21] S. Weinberg, Phys. Rev. **D26**, 287(1982).
- [22] P. Ball and R. Zwicky, Phys. Rev. **D71**, 014015(2005) [arXiv:hep-ph/0406232]; Phys. Rev. **D71**, 014029(2005) [arXiv:hep-ph/0412079].
- [23] J. G. Körner and G. A. Schuler, Phys. Lett. **B226**, 185(1989).
- [24] W. M. Yao et al., J. Phys. G **33**, 1(2006) and 2007 partial update for edition 2008.
- [25] Heavy Flavor Averaging Group, <http://www.slac.stanford.edu/xorg/hfag>.
- [26] C. H. Chen and C. Q. Geng, JHEP **0610**, 053(2006) [arXiv:hep-ph/0608166].
- [27] B. Aubert et al. (*BABAR* Collaboration), Phys. Rev. **D76**, 052002(2007).
- [28] K. Ikado et al. (Belle Collaboration), Phys. Rev. Lett. **97**, 251802(2006) [arXiv:hep-ex/0604018].
- [29] A. G. Akeroyd and S. Recksiegel, J. Phys. G **29**, 2311(2003) [arXiv:hep-ph/0306037].
- [30] M. Chemtob, Prog. Part. Nucl. Phys. **54**, 71(2005) [arXiv:hep-ph/0406029].
- [31] R. Barbier et al., Phys. Rept. **420**, 1(2005) [arXiv:hep-ph/0406039].
- [32] T. Hokuue et al. (Belle Collaboration), Phys. Lett. **B648**, 139(2007) [arXiv:hep-ex/0604024].

- [33] B. Aubert et al. (*BABAR* Collaboration), Phys. Rev. Lett. **98**, 091801(2007)
[arXiv:hep-ex/0612020].
- [34] B. Aubert et al. (*BABAR* Collaboration), Phys. Rev. Lett. **97**, 211801(2006)
[arXiv:hep-ex/0607089].
- [35] B. Aubert et al. (*BABAR* Collaboration), Phys. Rev. **D72**, R051102(2005)
[arXiv:hep-ex/0507003].
- [36] B. H. Behrens et al. (CLEO Collaboration), Phys. Rev. **D61**, 052001(2000)
[arXiv:hep-ex/9905056].
- [37] S. B. Athar et al. (CLEO Collaboration), Phys. Rev. **D68**, 072003(2003)
[arXiv:hep-ex/0304019].
- [38] B. C. Allanach, A. Dedes and H. K. Dreiner, Phys. Rev. **D60**, 075014(1999)
[arXiv:hep-ph/9906209].